

Geological and Geophysical Constraints Guide New Tectonic Reconstruction of the Gulf of Mexico

Irina Filina¹ and Erin Beutel²

¹University of Nebraska - Lincoln

²College of Charleston

November 22, 2022

Abstract

The Gulf of Mexico is a prolific petroleum basin with more than a century-long exploration history. Tectonic models proposed for the basin vary dramatically in many aspects, ranging from the pre-rift locations of the crustal blocks, the timing of the break-up to even the order of tectonic events. The reason for these disagreements is in a thick and complex overburden that obscures seismic imaging of crustal structures. To overcome that, we integrated seismic data with gravity and magnetic fields to determine the crustal architecture in different parts of the basin, as well as to map the location of the key tectonic features. The subsequent spatial analysis of potential fields allowed us to trace the tectonic structures outside of seismic coverage. As a result, a set of new geological constraints was derived including the Triassic rifts, regions of Seaward Dipping Reflectors (SDR), and Jurassic pre-salt sedimentary basins in the eastern Gulf of Mexico and along the Yucatan margin, and two distinct crustal zones in the oceanic domain. We ensure the pre-breakup alignment of the crustal blocks based on the mapped geological features on the conjugate margins. Our tectonic reconstruction takes into account an apparent temporal variability of the magmatic regime during basin formation that ranged from CAMP (\sim 200 Ma) to an ultra-slow amagmatic spreading during the initial stage of the GoM opening (\sim 165 Ma). Our reconstruction also includes a major ridge reorganization (\sim 152 Ma) associated with increased magmatic supply. This second phase of oceanic spreading ceased at early Cretaceous (\sim 135 Ma) based on published correlation analysis of seismic and well data. Overall, the tectonic reconstruction presented here takes into account previously known and newly derived geological constraints and integrates various geophysical datasets, namely seismic, gravity, and magnetics.

Geological and Geophysical Constraints Guide New Tectonic Reconstruction of the Gulf of Mexico

Irina Filina¹, Erin Beutel²

1 University of Nebraska – Lincoln, ifilina2@unl.edu

2 College of Charleston, BeutelE@cofc.edu

Abstract

The Gulf of Mexico is a prolific petroleum basin with more than a century-long exploration history. Tectonic models proposed for the basin vary dramatically in many aspects, ranging from the pre-rift locations of the crustal blocks, the timing of the break-up to even the order of tectonic events. The reason for these disagreements is in a thick and complex overburden that obscures seismic imaging of crustal structures. To overcome that, we integrated seismic data with gravity and magnetic fields to determine the crustal architecture in different parts of the basin, as well as to map the location of the key tectonic features. The subsequent spatial analysis of potential fields allowed us to trace the tectonic structures outside of seismic coverage. As a result, a set of new geological constraints was derived including the Triassic rifts, regions of Seaward Dipping Reflectors (SDR), and Jurassic pre-salt sedimentary basins in the eastern Gulf of Mexico and along the Yucatan margin, and two distinct crustal zones in the oceanic domain.

We ensure the pre-breakup alignment of the crustal blocks based on the mapped geological features on the conjugate margins. Our tectonic reconstruction takes into account an apparent temporal variability of the magmatic regime during basin formation that ranged from CAMP (~200 Ma) to an ultra-slow amagmatic spreading during the initial stage of the GoM opening (~ 165 Ma). Our reconstruction also includes a major ridge reorganization (~ 152 Ma) associated with increased magmatic supply. This second phase of oceanic spreading ceased at early Cretaceous (~ 135 Ma) based on published correlation analysis of seismic and well data. Overall, the tectonic reconstruction presented here takes into account previously known and newly derived geological constraints and integrates various geophysical datasets, namely seismic, gravity, and magnetics.

1. Introduction

The Gulf of Mexico (GoM) is a petroleum-rich basin located on the southeastern edge of North America (**Figure 1**). The basin has a more than a century-long exploration history (Galloway, 2008) that resulted in multiple wells, primarily targeting oil and gas deposits within a sedimentary section. The thickness of sediments exceeds 14 km (Laske et al., 2013), so the pre-GoM Paleozoic rocks and/or the basement are sampled only by a small number of wells around the rim of the basin (**Figure 1A**; Scott et al., 1961; Ramos, 1975; Ball et al., 1988; Dobson and Buffler, 1991; Woods et al., 1991; MacRae and Watkins, 1995; Coombs et al., 2019; Erlich and Pindell, 2020). The vast majority of geophysical data acquired in the basin is proprietary, although several seismic sections, such as the ones shown in **Figure 2** (Snedden et al., 2014; Lin et al., 2019, Filina et al., in review), are recently published and are available for qualitative analysis for a general geoscience community.

The tectonic history of the basin remains poorly understood even if the new high-quality data are constantly being collected (e.g., Saunders et al., 2016; Horn et al., 2017; O'Reilly et al., 2017; Deighton et al., 2017) and new wells are being drilled in deepwater in both U.S and Mexican sectors. Many tectonic models of the Gulf of Mexico opening are proposed in the literature, but they are contradictory to each other in some aspects as is summarized in Filina et al. (in review). The overall consensus implies that the formation of the basin relates to the disassembly of the supercontinent Pangaea that started in the Late Triassic. The oceanic spreading initiated in the Late Jurassic and ceased in the Early Cretaceous as the Yucatan crustal block rotated away from North America. However, several controversies in tectonic history are still not resolved. These include the tectonic affiliation of the Triassic redbeds (earlier syn-rift or post-collisional sedimentary basin), the nature of rifting and breakup (magma-rich vs magma-poor), the timing of salt deposition with respect to the formation of oceanic crust (i.e., what was first), and the pre-rift location of the crustal blocks. The primary reason for these disputes is the poor seismic image of crustal structures, especially in the continental domain and over the ocean-continent transition zone, which allows for multiple, sometimes contradicting interpretations. To overcome that, integration with other datasets, particularly potential fields (**Figure 3**), is necessary. In this paper, we describe how the joint analysis of publicly available seismic data with potential fields (gravity and magnetic) and observed lithospheric seismicity (**Figure 1B**) helps delineating subsurface structures that honor all the data. We review published integrated models and summarize the key tectonic features mapped by those models, such as the Ocean-Continent boundary (OCB), various magmatic complexes, pre-salt sedimentary basins, and two distinct crustal zones in the oceanic domain. We then perform a spatial analysis of potential fields to trace these structures outside of the models' coverage. We use these mapped geological features as constraints for the new tectonic reconstruction of the basin. Our integrated approach allows for a more confident tectonic reconstruction as geological structures at the conjugate margins end up being aligned when restored to their pre-break-up locations.

2. Geologic History

Major tectonic events leading to the formation of the Gulf of Mexico are illustrated in **Figure 4**. The basin opened to the south of the Ouachita-Marathon orogenic belt that marks the assembly of the supercontinent Pangaea that was completed by middle Permian (Soto-Kerans et al., 2020). The orogenic belt is easily traceable in potential fields to the north of the GoM (marked with red arrows in **Figure 1A**). Pre-GoM Paleozoic rocks were penetrated by some wells mostly at the northern edge of the basin (**Figure 1A**).

The Pangea disassemble started in Triassic, with the South Georgia Rift system (**Figure 5A**; McBride, 1991) that failed and is known to be capped by the flood basalts of the Central Atlantic Magmatic Province (CAMP) that occurred ~ 200 Ma (e.g., Marzoli et al., 1999; McHone, 2003). The overlying Triassic redbeds, such as Eagle Mills Formation (the name comes from the well in southern Arkansas) are penetrated by multiple wells in the northern part of the basin (**Figure 1A**). The palynology analysis allowed to date these redbeds as Carnian (~237 Ma, Wood and Benson, 2000). In the southern GoM, the Eagle Mills equivalents include several formations of the Huizachal Group (Barboza-Gudiño et al., 2010; Martini and Ortega-Gutiérrez, 2016), although some of them are overprinted by the tectonics of the East Mexico Permo-Triassic Nazas arc (Stern and Dickinson, 2010).

Deposition of salt (shown with pink outlines in **Figure 1A**) - plays a significant role in the majority of published tectonic reconstructions. Until 2019, the age of salt was thought to be Callovian (~166 - 163 Ma) based on the stratigraphy (Salvador et al., 1991), while recently the earlier Bajocian (~170 - 168 Ma) salt age is confirmed with Sr isotopes, so some models now have to readjust the timing of major tectonic phases (Pindell et al., 2020). Most authors suggest that the salt was deposited at the last stage of continental rifting (e.g., Eddy et al., 2014; Nguyen and Mann, 2016), while Hudec et al. (2013) argue for 7 to 12 Myr of post-salt continental stretching in the central part of the basin prior the oceanic spreading. Recently, several authors proposed that salt deposition was coincident with an oceanic spreading (Kneller and Johnson, 2011; Lundin and Doré, 2017; Pindell et al., 2020), while some even allow salt deposition in two separated basins after the oceanic crust was formed (Padilla y Sánchez, 2016).

Despite the published models agree that the GoM opened via counterclockwise rotation of the Yucatan crustal block, details of this rotation vary dramatically between them. Some models utilize paleomagnetic data for Mexican outcrops to constrain the total degree of rotation of the Yucatan crustal block that varies in the literature from >70 deg (Molina-Garza et al., 1992) to ~40 deg (Godínez-Urban et al., 2011a, b), and consequently does not provide a solid constrain. The proposed location of conjugate margins also varies between the models. Such, the study of Van Avendonk et al. (2015) concludes that Texas and western Yucatan margins are conjugates based on the tectonic reconstruction that results in a tight fit of the crustal blocks. Alternatively, a companion paper of Eddy et al. (2014) suggests that the Louisiana margin is conjugate for the western Yucatan. In contrast, Lundin and Doré (2017) reconstruct the western Yucatan to northeastern GoM (Alabama margin), while Hudec and Norton (2019) report on the outer troughs mapped in northern Yucatan and Florida are conjugate features. In our study, we map matching geological features on both U.S. and Mexican margins based on the integration of multiple geophysical data to constrain the tectonic reconstruction of the basin.

The timing of the drifting phase ranges drastically in the literature because of the uncertainty in geologic interpretations (the start of drifting varies from 190 to 154 Ma among different papers, while the end of oceanic spreading ranges between 154 and 128 Ma). For example, Lundin and Doré (2017) interpret strong magnetic anomalies aligned with the basinward dipping reflectors in the northeastern GoM as evidence of subaerial basalt flows (referred to as SDR - seaward dipping reflectors) based on a similar appearance of these complexes to the drilled SDRs in Norway and Greenland (e.g., Hinz, 1981; Mjelde et al., 2008). They further expand this interpretation to other pronounced magnetic anomalies around the GoM (**Figure 3B**) despite the seismic imaging in that part of the basin is very challenging and no basinward dipping reflections are observed in seismic data. Lundin and Doré (2017) thus conclude a magma-rich nature of the GoM breakup and interpret all strong positive magnetic anomalies surrounding the basin as SDR complexes, which guide their tectonic restoration (yellow polygons in **Figure 1B**). Multiple authors interpret the basinward dipping reflectors observed in the northeastern and southern parts of the basin as evidence of magma-rich basin breakup (Imbert and Post, 2005; Imbert et al., 2005; Eddy et al., 2014; Liu et al., 2019; Filina and Hartford, 2021). In contrast, the model of Minguez et al. (2020) suggests that the strong magnetic signature of Louisiana magnetic anomaly (labeled as 4 in **Figure 3B**) can be modeled without any magmatic SDR complex, thus arguing for a magma-poor breakup. In this study, we support the evidence of the magmatic addition during the rifting stage (not at the break-up as in Lundin and Doré, 2017) based on modeling of magnetic data in various parts of the basin that requires the presence of highly magnetic rocks in the subsurface in order to explain observed magnetic anomalies. We also acknowledge the time constraints on the tectonic events from Snedden et al. (2014) that are based on seismic reflection data tied

to industry wells with biostratigraphy markers, namely the initiation of spreading at ~160 Ma and the end of the oceanic crust formation at ~137 Ma.

In addition to pre-CAMP South Georgia Rift system (**Figure 5A**), several major tectonic structures are mentioned in the literature, such as outer trough (Hudec and Norton, 2019) and BAHA high (Hudec et al., 2020; the acronym comes from the exploration prospects along the high). The outer troughs represent the regions of a sudden up to 2 km deep drop in the basement boundary with evidence of unconfined salt flow together with an overlying Jurassic sedimentary section that are mapped by Hudec and Norton (2019) from proprietary seismic data on the Yucatan and Florida margins (**Figures 2A** and **5A**). Filina and Hartford (2021; **Figure 5F**) interpreted this feature to be related to exhumation of the lower crust that occurred at the final, post-salt stage of continental rifting. Another intriguing crustal feature in the GoM is the BAHA high in the west (**Figure 5A**) as the nature of the crust there remains highly debated. Fiduk et al. (1999) suggest extended continental crust in that region based on multiple linear basement highs that were interpreted as horsts marking the tilted blocks. In contrast, Minguez et al. (2020) describe this region as exhumed upper mantle based on the magnetic signature. Alternatively, Hudec et al. (2020) argue that the crust of BAHA high is volcanic (i.e., oceanic) in origin, and it was emplaced at the time of salt deposition. In our study, we interpret this region as an oceanic crust produced in the initial spreading phase (**Figures 4, 5 and 6**), which is consistent with the crustal thickness determined by refraction data of Nakamura et al. (1988). Another structure that worth mentioning is the basement ramp (Hudec et al., 2013) - the step-up of the oceanic basement with respect to the continental one, that was interpreted by Hudec et al. (2013) from proprietary seismic data as a marker for the limit of oceanic crust (shown with pink color in **Figure 1B**). The later interpretations of Hudec's team conclude that the nature of the crust around the ramp remains poorly understood (Curry et al., 2018; Hudec and Norton, 2019). Moreover, Curry et al. (2018) outline a region of "uncertain crust" generally coincident with the ocean-continent boundary. Many of the integrated models shown in **Figure 5** acknowledge this step-up of oceanic crust with respect to the continental basement.

Multiple authors mapped the segments of the extinct spreading centers and corresponding transform faults in the center of the basin based on gravity data (**Figures 1** and **3A**). Despite these interpretations are done on the same dataset, the mapped tectonic features still show discrepancies exceeding 60 km. The drastic asymmetry of the basin with respect to the spreading center should also be noted (**Figure 1A**), which is especially apparent in the eastern part of the basin where the crustal domain to the north of the spreading center is noticeably wider than the one to the south. Some models suggest that this results from an asymmetric spreading (Hudec et al., 2013; Nguyen and Mann, 2016). In our model, we explain this apparent asymmetry with two distinct spreading episodes, namely the initial one from ~ 165 Ma that produced thin crust adjacent to the OCB in many parts of the basin, including the crust of BAHA high in the northwestern GoM and the northmost zone of oceanic crust in the northeastern GoM (**Figures 5** and **6**). The second spreading episode follows the major ridge reorganization~ 152 Ma and produces thicker and layered crust until ~ 135 Ma (**Figure 4**). We utilize pronounced gravity lows to map the two sets of spreading centers that further guide our tectonic reconstruction.

3. Integrated Geophysical modeling

The concept of integrated geophysical modeling assumes multiple geophysical and geological observations jointly analyzed in order to derive the subsurface model that honors all of them. In this study, we utilize 2D seismic reflection sections (such as the ones shown in **Figure 2**), seismic refraction data (Ewing et al., 1960; Ibrahim et al., 1981; Nakamura et al., 1988; Eddy et al., 2014, 2018; Christeson et al., 2014; Van Avendonk et al., 2015), gravity (Sandwell et al., 2014; **Figures 1 and 3A**) and magnetic fields (Bankey et al., 2002; Meyer et al., 2017; Minguez et al., 2020; **Figure 3**), as well as limited core data to constrain physical properties of subsurface rocks (i.e., Schlager et al., 1984; Hilterman, 1998). An example of an integrated geophysical model is shown in **Figure 3C**.

- **Northwestern GoM (GUMBO1)**

The model in the northwestern GoM (**Figure 5B**) follows the seismic refraction line GUMBO1 (Van Avendonk et al., 2015) that images a complex subsurface consisting of a highly variable sedimentary cover with multiple salt structures over a crustal layer with several high-velocity zones ($V_p > 7.5$ km/s). The structures imaged in this profile are interpreted differently by various authors. Lundin and Doré (2017) position the entire profile over the oceanic domain. Van Avendonk et al. (2015) suggest thinned and hyperextended continental crust with a ~40 km wide zone of interpreted exhumed mantle adjacent to oceanic crust (the last 80 km of the profile) that is overlain by salt and thins basinward from 9 to 5 km. Filina (2019) noticed that the seismic refraction results of Van Avendonk et al (2015) lack a thick salt structure, known as “salt wall” associated with the Perdido fold belt (Filina et al., 2015; this feature is evident in gravity data and is labeled with “1” in **Figure 3A**). The absence of this thick salt in the velocity model results in distorted crustal seismic velocities. Reinterpreted refraction data, further integrated with potential fields, revealed thinned and intruded continental crust (Filina, 2019; **Figure 5B**) that varies in thickness from ~15 km in the northwestern end of the line to ~10 km near the OCB located basinward of the “salt wall” near the Sigsbee Escarpment. The crust at the southwestern edge of the line, over the BAHA high, is interpreted to be oceanic with a total thickness of 6 km, which is consistent with the refraction data of Nakamura et al. (1988), and with the conclusion of Van Avendonk et al. (2015). The high-velocity zones are interpreted as magmatic intrusions presumably emplaced during continental rifting as they require high magnetic susceptibilities to explain observed magnetic signatures.

Our interpretation (**Figure 5B**) suggests no pre-salt sediments deposited in the northwestern GoM (see more details in Filina, 2019). This conclusion is consistent with the results of the 3D seismic survey described by Filina et al. (2015) in the northwestern GoM that was reprocessed with guidance from 3D gravity modeling. The integration with gravity resulted in significantly improved seismic imaging and ultimately allowed to map the acoustic basement, revealing no pre-salt sediments in the area.

- **Central GoM (GUMBO2)**

The north-central GoM is sampled by a seismic refraction line GUMBO2 (Eddy et al., 2018) that is generally aligned with seismic reflection line GULFSPAN 2000 (Radovich et al., 2011). All but two published tectonic models agree that the northern end of the line is located over the stretched continental crust (**Figure 1B**), although the location of the OCB varies between the models up to 149 km (87 mi) in that region. Kneller and Johnson (2011) and Lundin and Doré (2017) are the only authors proposing that the entire line is over the oceanic domain (**Figure 1B**). OCB suggested by Eddy et al. (2018) is located near the Sigsbee Escarpment, which was validated by an integrated geophysical analysis by Filina (2019), concluding that the OCB near the Sigsbee (**Figure 5C**) is preferable to explain observed gravity and

magnetic anomalies. However, this OCB challenges many published tectonic models that assume a tight fit between western Yucatan and the northern GoM margin, demanding the OCB to be much more landward than it is suggested by the GUMBO2 results (compare OCBs in **Figures 1B** and **5A**).

Similar to other GUMBO lines, several high-velocity zones in the lower crust that are aligned with strong magnetic anomalies are interpreted as magmatic complexes that were emplaced presumably during the continental rifting phase. No pre-salt sediments are concluded for the GUMBO2 line as well as they are no evident neither in seismic reflection nor in seismic refraction data, and they are not demanded by potential fields. The absence of the pre-salt deposits in the northwestern and central GoM is consistent with the observations of Ewing and Galloway (2019) about a general lack of early Jurassic deposits in the northwestern GoM, as well as with the regional uplift in Texas in Late Triassic - Early Jurassic that was documented by Dickinson et al (2010).

- **Northeastern GoM (GUMBO3, GUMBO4)**

There is much better agreement between published OCBs in the northeastern GoM (**Figure 1B**). However, the nature of the margin, i.e., magma-rich vs. magma-poor, is highly debated in the literature. Both landward and basinward dipping reflectors are imaged in seismic in this area that are interpreted by various authors either as magmatic complex (SDR) associated to magma-rich margin (e.g., Imbert and Post, 2005; Imbert et al., 2005; Eddy et al., 2014, Liu et al., 2019) or like growth faults filled with sediments related to magma-poor basin formation (Rowan, 2014, Curry et al., 2018, Minguez, 2020). Liu et al. (2019) performed an integrated geophysical analysis of several seismic reflection and refraction lines at the northeastern part of the basin and established two regions of the seismic dipping reflectors that require high densities and high magnetic susceptibilities to explain the observed gravity and magnetic fields (see an example in **Figure 5D**). The northern complex (referred to by Liu et al. (2019) as the Northern SDR) is aligned with the Apalachicola Basin (labeled as “AB” in **Figures 5A** and **5D**). We interpret this structure as a buried continuation of the Triassic South Georgia Rift System, which is known to be capped by the CAMP volcanics (McBride, 1991). Therefore, we interpret the highly magnetic rocks in that region demanded from the observed magnetic signature as evidence of CAMP-related magmatism. The second magmatic complex to the south (**Figure 5D**, referred to by Liu et al. (2019) as the Southern SDR) is also aligned with the basinward dipping reflectors in seismic data and also requires high densities and magnetic susceptibilities to match potential fields. As already mentioned, this is interpreted as an SDR complex by many authors, although the timing of this structure remains discussed in the literature (Eddy et al., 2014; Lundin and Doré, 2017). In our reconstruction, we associate these complexes with the CAMP magmatic event (~ 200 Ma, **Figure 4**), i.e., they were emplaced during the continental rifting phase (not at the break-up phase as is suggested by other authors). This interpretation agrees with several high-velocity zones in the lower crust imaged by several lines GUMBO lines (**Figures 5B-E**) representing igneous intrusive bodies emplaced at the same time during a magma-assisted continental rifting phase. This conclusion is also consistent with multiple basaltic igneous rocks encountered from the wells in the shallow waters and onshore in this region (**Figure 1A**) as well as with the findings of the DSDP Leg 77 wells offshore Yucatan (Schlager et al., 1984) that encountered diabase intrusions with Jurassic crystallization age in Paleozoic metasediments. The mapped magmatic complexes, particularly SDRs, are further used as constraints in our tectonic reconstruction as they are aligned with a similar structure at the conjugate margin (**Figures 5 and 6**).

- **Yucatan margin**

Filina and Hartford (2021) developed three integrated models (**Figures 5F-H**) along the seismic lines published by Williams-Rojas et al. (2012). Multiple seismic sections at the Yucatan margin show basinward dipping reflectors (Williams-Rojas et al., 2012; Saunders et al., 2016; O'Reilly et al., 2017; Steier and Mann, 2019), similar to the ones seen in **Figure 2B**, that are further aligned with pronounced magnetic anomalies (labeled as “4” in **Figure 3B**). The magnetic signature for the profile shown in **Figure 5F** requests a presence of two anomalous bodies - one shallow (i.e., of a shorter wavelength) consistent with an SDR complex, and one deeper one located slightly basinward, interpreted as a “feeding” intrusive body (Filina and Hartford, 2021). In addition to the magmatic SDR complexes that are interpreted at both Yucatan and eastern GoM margins (**Figures 5D-F**), several other matching geological structures are mapped at both locations. Hudec and Norton (2019) outlined up to 2 km deep outer troughs from proprietary seismic data on both margins (**Figures 2B** and **5A**); this feature is wider on the Yucatan side (~ 40 km) and is less than 20 km wide in the northeastern GoM (Hudec and Norton (2019) refer to that as to Florida margin). Integrated analysis of seismic and potential fields data (Filina and Hartford, 2021) for the profile shown in **Figure 5F** suggests that the outer trough is underlain by exhumed lower continental crust. The exhumation has likely occurred at the very last (post-salt) phase of continental rifting (as in Hudec et al., 2013). The removal of the low-density upper crust immediately before the oceanic spreading triggered the rapid subsidence of that part of the margin that, in turn, triggered the unconfined salt flow documented by Hudec and Norton (2019). A similar region of nearly exhumed lower continental crust may be interpreted in the northeastern GoM (**Figure 5E**, ~ 10 km thick region of $V_p \sim 7$ km/s adjacent to OCB, Christeson et al., 2014). This interpreted exhumation of lower continental crust is consistent with an estimated ultra-slow spreading rate (0.9 cm/yr, Filina et al., 2020), as well as with the geochemical analysis of the volcanic rocks encountered in salt diapirs, that have post salt crystallization age (~ 160 Ma) and originate from the deprived magmatic source (Stern et al., 2011). The rapid marginal collapse is also documented in the northeastern GoM from proprietary seismic data by Pindell et al. (2014), although is attributed to the exhumation of the upper mantle rather than the lower continental crust. However, the integration of seismic data with potential fields does not support mantle exhumation in the GoM (**Figure 5**). In addition, seismic data (Eddy et al., 2014; Christeson et al., 2014) show a strong reflection and an abrupt velocity contrast associated with the Moho boundary that are not consistent with a mantle exhumation.

The thick pre-salt sedimentary basins represent other matching tectonic features on the Yucatan and the northeastern GoM margins (**Figure 5**). These sediments were first documented at the Yucatan margin by Williams-Rojas et al. (2012), who presented a convincing seismic section with up to 5 km thick sediments imaged beneath the salt, although the base of these pre-salt deposits was not confidently mapped in seismic reflection data. Filina and Harford (2021) combined seismic and potential fields to outline up to 100 km wide pre-salt sedimentary basin in the Yucatan margin (**Figure 5F-H**) that can be also seen in seismic data in **Figure 2B** as well as in the regional seismic reflection profile of Horn et al. (2017) and in the corresponding models (**Figures 5J** and **5K**).

Oceanic domain

The GUMBO experiment (Eddy et al., 2014, 2018; Christeson et al., 2014) revealed that oceanic crust in the GoM shows significant variations both in thickness (ranges between 5 and 9 km) and in physical properties (V_p ranges from 5.5-6 km/s to >7 km/s). The changes in the GoM oceanic crust are evident in seismic reflection data in **Figure 2** and interpreted in many models in **Figure 5**. The thickness of the crust in those models are not only constrained by seismic reflection data (as the ones shown in **Figure 2**) but also by vintage refraction data (Ewing et al., 1960; Ibrahim et al., 1981; Nakamura et al., 1988) that are shown

as blue columns in the cross-sections of **Figure 5** (see the locations of seismic refraction constraints in **Figure 5A**). Overall, two distinct crustal zones in the eastern GoM are identified (**Figure 5A**): thinner and uniform crust near the OCB and thicker and layered one in the center of the basin. The thicknesses and physical properties are guided by seismic refraction data of Eddy et al., 2014, 2018; Christeson et al., 2014, and the observed crustal variations are validated with observed gravity and magnetic fields. We refer to the contact between the two oceanic crustal zones as to pseudofault. We map that structure in five profiles in **Figure 5** (marked with yellow circles).

4. Spatial analysis of gravity and magnetic data and mapped tectonic features

Potential fields - gravity and magnetic - are sensitive to variation in physical properties of subsurface rocks, namely in density and magnetic susceptibility. The major geological structures, such as the boundary between continental and oceanic crusts, are associated with significant contrasts in these properties, thus allowing us to map these structures from the filtered gravity and magnetic data.

In gravity, we computed the Bouguer correction based on densities of water and the top sediments (**Figure 5**). We then computed the regional trend via an upward continuation of the Bouguer gravity anomaly to an elevation of 40 km. We chose this value by trial and error as the one removing high-frequency components in gravity due to shallower subsurface structures, so the resultant regional trend represents the broad and smooth signal from deep regional sources. In magnetics, we performed differential RTP to correct for the skewness of observed anomalies due to non-vertical ambient field. We then found a regional magnetic trend via upward continuation to an elevation of 25 km. This lower elevation was used because the magnetic field decreases faster with distance than gravity (Telford et al., 1990). Once we remove the regional trends from both gravity and magnetic fields, we have applied the tilt derivative filter (Salem et al., 2008) to highlight the regions where the residual fields change the most (**Figures 6A** and **6B**).

- **Ocean-Continent Boundary (OCB)**

The OCB was determined in all models (blue markers in **Figures 2, 5, and 6**). As this boundary is associated with a significant contrast in the physical properties of continental and oceanic rocks, it corresponds to signals in both potential fields – a pronounced high in gravity and a high-trough pattern in magnetics (**Figures 3A and 3B**). This correlation allowed us to trace the OCB confidently for the entire basin (**Figures 5A and 6**). The fact that our analysis integrates multiple geophysical datasets gives us confidence in the derived OCB location (to be compared to multiple interpretations in **Figure 1B**).

- **Pre-salt basins**

The pre-salt basins are identified in the northeastern and southern parts of the Gulf of Mexico (**Figures 2, 5, and 6**). The presence of thick pre-salt deposits is evident in multiple seismic cross-sections (Williams-Rojas et al., 2012; Saunders et al., 2016; Horn et al., 2017; Liu et al., 2019; Lin et al., 2019), although these sediments have not been drilled and their age remains unconstrained to date. We model this section as dense and slightly magnetic sediments (**Figure 5**) to account for their inferred volcaniclastic nature, which is further validated by a good match between observed and computed potential fields (Liu et al., 2019; Filina and Hartford, 2021). Noticeably, a thick pre-salt section is only interpreted in the northeastern and southern parts for the Gulf of Mexico (**Figures 5 and 6**), while no these sediments are observed in the northwestern and central GoM (**Figure 5B** and **5C**), which potentially relates to the Late Triassic- Early Jurassic uplift

in Texas (Dickinson et al., 2010) that prevents these sediments from being deposited in those regions. We utilize the mapped pre-salt basins in the northeastern GoM and at the Yucatan margin as conjugate features formed at the stretched continental crust after the CAMP event (i.e., in the early Jurassic) and use them as constraints for our tectonic reconstruction at that time.

- **Oceanic domain - two spreading episodes and pseudofault marking the contact between them**

Our modeling (**Figure 5**) suggests the presence of two distinct spreading episodes in the Gulf of Mexico that produced drastically different oceanic crusts. The one immediately adjacent to the OCB is thin (~ 5 km) and uniform (i.e., modeled as a single layer) based on seismic velocities $V_p \sim 7$ km/s determined by refraction data of Christeson et al. (2014). We interpret this crust to be produced by an initial ultra-slow spreading episode (~165-152 Ma) with an estimated spreading rate of 0.9 cm/yr (Filina et al., 2020). At ~152 Ma, the ridge reorganization occurred that resulted in the NE-SW trending spreading centers (thick black lines in **Figure 5A**) that are evident in gravity data (**Figures 1** and **3A**). The oceanic crust produced in the second spreading episode (~152 -135 Ma) is thicker (up to 9 km) and has two layers (Eddy et al., 2014), which are interpreted as basalts ($V_p \sim 5.5$ - 6 km/s) over gabbro ($V_p \sim 7$ km/s). Despite an apparent increase in the availability of magmatic material during the younger spreading episode, the spreading rate remained slow (estimated full rate of 1.1 cm/yr; Filina et al., 2020). The pseudofault - the boundary between the two crustal domains - can be traced in both filtered potential fields as an apparent change in character (**Figure 6**). This boundary is further aligned with the hypocenters of several recent earthquakes (Filina et al., 2020), suggesting that the pseudofaults in the eastern GoM represent zones of weakness that are currently being reactivated under compressional stress.

Our tectonic reconstruction (**Figure 7**) accounts for this two-phased formation of oceanic crust. The ridge reorganization during the formation of oceanic crust at ~152 Ma explains multiple puzzling geological observations, namely 1) the severe asymmetry in the oceanic domain (**Figure 1A**), 2) the presence of two distinct crustal zones with dramatically different thickness and physical properties (**Figure 5**), and 3) the observed seismicity within the oceanic domain that is not aligned with any known tectonic structure (Filina et al., 2020).

- **Magmatic addition**

Many of our models (**Figure 5**) suggest the presence of igneous magmatic complexes within the crust, such as the SDRs in the northeastern and southern margins, and multiple intrusive bodies in the lower crust all over the basin. The latter are aligned with high seismic velocities imaged from refraction profiles in the northern Gulf of Mexico (Eddy et al., 2014, 2018; Christeson et al., 2014; Van Avendonk et al., 2015) and with strong magnetic anomalies (**Figure 3B**). As already mentioned, many authors interpret those as rift-related magmatic addition (Eddy et al., 2014, 2018; Christeson et al., 2014; Filina, 2019; Liu et al., 2019). These features must be made of dense and highly magnetic rocks in order to explain observed gravity and magnetic anomalies. Moreover, the shallow magmatic complexes (referred to as SDRs) are aligned with the basinward dipping reflectors observed in seismic (such as the ones in **Figure 2A**). Their interpretation as rift-related magmatic addition is also consistent with the findings of the DSDP Leg 77 well (**Figure 1A**; Schlager et al., 1984) that sampled Paleozoic basement intruded by diabase dike with Early Jurassic crystallization age.

The extents of the SDR provinces were established from our spatial analysis (**Figure 6**) as up to 400 km long and up to 50 km wide in the Yucatan margin, while this complex appears to be shorter (~ 270 km) in

the northeastern part of the basin. We used the mapped SDR complexes as conjugate features on both margins to constrain the tectonic reconstruction of the Early Jurassic time. In general, we conclude that the availability of magmatic material varied throughout the history of the basin from magma-rich CAMP (presumably responsible for the observed SDRs and igneous intrusions) to amagmatic post-salt continental stretching that resulted in the exhumation of the upper crust in Yucatan (**Figure 5F**) and northeastern GoM (**Figure 5E**) that was followed by an ultra-slow spreading producing thin oceanic crust \sim 165 -152 Ma. The magmatic input apparently increased after ridge reorganization at \sim 152 Ma, as thicker than normal oceanic crust (**Figures 5D-E** and **5I-K**) was produced in the second spreading episode (\sim 152-137 Ma). These temporal variations in the magmatic input are consistent with observations of Planke et al. (2000) who showed that the periods of significant magmatic addition may alternate with episodes of very limited volcanism in passive continental margins.

5. Tectonic reconstruction of the basin

The extensive interpretation and identification of geologic features in the previous sections is used as a framework for the tectonic reconstruction of the Gulf of Mexico (**Table 1**). Particularly, we utilize the matching tectonic features at both margins, namely the Triassic basins (labeled “2” in **Figure 3**) and SDR complexes for the Late Triassic reconstruction (**Figures 7A and 7B**), the pre-salt sedimentary basins for the Early and Middle Jurassic ones (**Figures 7C-7E**), the evidence of the exhumation of the lower continental crust at the final (post-salt) stage of continental rifting (**Figure 7F**), and the two phases of oceanic spreading (**Figures 7F-7H**) for late Jurassic -Early Cretaceous times. While our reconstructions are guided by these tectonic constraints, they have also relied heavily on our understanding of the deformation seen in the crust itself.

Each rift basin evolves differently depending on the magma supply, the initial thickness of the crust, pre-existing weaknesses, and the orthogonality of the extension to pre-existing weaknesses, but overall, continental rifts follow a pattern during their evolution. Continental rifts generally start with widespread deformation, that is followed by the localization of deformation to a narrow zone leading to the formation of thinned transitional crust, and, eventually, to the formation of oceanic crust (e.g., Guan et al., 2019; Corti, 2012). No matter the angle of interaction or the presence or absence of magma, the ability of the two sides of the rift to influence the stress state of each other is greatly reduced once the transitional stage is reached. However, there must still be some connection between the two sides of the rift because the continental crust is still extending.

We used the program GPlates2.2.0 along with the Mueller et al. (2019) tectonic reconstruction data as a starting point for our reconstruction of the opening of the Gulf of Mexico. We then modified the motion of the Yucatan/Chiapas (henceforth referred to as Yucatan) and the Suwanee-Carolina Terrane (henceforth referred to as the Florida Block) based on the geophysical and tectonic structures listed in **Table 1**. Each time period had its own unique set of variables used in the reconstruction, but the basic principle of the reconstruction is that the similarly aged unique features likely formed adjacent to each other and that the relative motion of the plates must create a stress field that matches the observed deformations. However, large-scale regional features rarely create straight lines or match perfectly during tectonic deformation as each individual basin, rift, fault, magmatic complex, and stress responds to the local conditions in the

context of the larger tectonic picture. The poles of rotation derived from our reconstruction are listed in **Table 2**.

Initial Configuration

While the amalgamation of Pangea and the many questions that remain about the origins, docking times, and the locations of sutures for the various southeastern terranes are beyond the scope of this paper, there are some generalizations we assume. The southeastern corner of Laurentia is currently composed of a series of terranes that docked during the formation of Pangea (e.g., Netto and Dunbar, 2019) some of those terranes remained with North America during the break-up of Pangea (e.g. Sabine, Suwanee, and Carolina), while others like the Yucatan acted as microplates and were pulled away from North America when Pangea broke apart (e.g. Zhao et al., 2020). We begin our reconstruction at ~230 based on the age of the first extension of the Triassic rifts in southeastern North America (Labails et al., 2010).

Late Triassic (230-205 Ma, pre-CAMP)

The supercontinent Pangea began to slowly separate around 230 Ma (e.g., Traverse, 1987; Labails et al., 2010; Frizon de Lamotte et al., 2015; Leleu et al., 2016; Peace et al., 2020), resulting in continental rifting in southeastern North America including Florida and the Yucatan blocks, two of the several terranes accreted during the assembly of Pangea (Soreghan and Soreghan, 2013). The associated Triassic redbeds are documented on both sides and are penetrated in many wells in the northern margin (**Figure 1A**), as well as studied from outcrops in Mexico (Barboza-Gudiño et al., 2010; Martini and Ortega-Gutiérrez, 2016). While small regional variations in rift orientation and structure are common in continental rifting, the rifts of approximately the same age in the same region should have approximately the same orientation (e.g., Peace et al., 2016). Therefore, we lined up the Triassic rifts from the northern margin of the Yucatan block with the rifts of the same age along the eastern shore of Florida that are apparent in potential fields (**Figure 3**) in our Late Triassic reconstruction (**Figure 7A**).

We have also used the known motions of the larger plates at this time to determine the location and motion of the Yucatan (Mueller et al., 2019). Specifically, any reconstruction must result in plate motions that would produce the observed deformation from that time period. The NE-SW trending Triassic rifts in Florida that match the Yucatan rifts also are oriented similarly to the South Georgia Rift (**Figure 5A**) and other rifts in Georgia and South Carolina (**Figure 7A**; Heffner et al., 2012; Heffner 2013; Marzen et al., 2020; Pindell et al., 2020). These rifts all contain sediments indicating an age of origin ~ 230 Ma (e.g., Labails et al., 2010), therefore, they all must be related to the same tectonic deformational event. As shown in **Figure 7A**, the relative motion of the southeastern corner of North America to South America and Africa would likely produce basins of this orientation. Therefore, both the Yucatan block and Florida block were a) located at the Southeastern corner of North America, b) connected enough to North America to be affected by its motion, and c) connected to South America/Africa. However, to account for the stretching of the continental crust, both the Yucatan and Florida terranes are modeled as moving very slightly to the southeast (**Figure 7A**). This statement is based on the assumption that the stress (motion) is not transmitted well across weak boundaries. Therefore, in order to create the rift basins in Yucatan and Florida, both needed to be strongly connected to the surrounding continents. Thus, they will continue to be affected on a large scale by the motions of the larger continents until there is a weak zone between them.

Based on the South Georgia Rift, the NE-SW oriented rifting due to NW-SE tensional stresses continued until around 205 Ma, at which time the South Georgia Rift appears to have shut off (e.g., McBride, 1991; Marzen et al., 2020). This timing agrees with the observation that the CAMP magmatic complexes (~ 200 Ma) in the South Georgia Rift are not faulted (McBride, 1991; Marzen et al., 2020). Therefore, the plate motion between North America, the Yucatan, the Florida Block, and Gondwana was likely fairly steady between 230 Ma and 205 Ma, and both the Yucatan and Florida blocks were likely relatively stationary. There are very few Triassic continental rifts similar to what is seen in Florida and the South Georgia rift to the west of the Mississippi (Snedden and Galloway, 2019), suggesting that the tie between South America and North America was either very weak and/or the deformation was accommodated within the suture zone north of the Sabine terrane (Huerta and Harry, 2012; Keller et al., 2016).

Reconstruction of the Chiapas block is fraught with numerous interpretations overprinted by multiple collisions (e.g., Pindell et al., 2020). In our model, we reconstruct it as being attached to the Yucatan and embedded in southern North America (**Figure 7A**). This area was identified by Thomas (2006) as being a significant embayment into the North American continent because of the rifting in the late Precambrian. Therefore, we have put the Chiapas terrane into the embayment, it could be in the open area between South America and North America below what is now Texas, however, there is no data on land suggesting a different stress field than that generated by the rotation of the Yucatan.

Late Triassic- Early Jurassic (205-195 Ma)

The CAMP massive igneous intrusion marks the end of the Triassic with injected dikes, sills, and basaltic flows from the northern parts of South America and Africa to Iberia. Modern dating suggests that it mostly occurred within 1 million years around 200 Ma (e.g., Nomade et al., 2007; Marzoli et al., 2018), but that there may have been later pulses. The older dating of what is now known as the CAMP complexes came up with the earlier age ~ 180 - 190 Ma that was later amended to around 200 Ma (Nomade et al., 2007; Lanphere and Gohn, 1983; Gottfried et al., 1983). We, therefore, hypothesize that the ~ 190 Ma dates of the diabase intrusions from the DSDP wells (Schlager et al., 1984) may be off, and the encountered magmatism indeed relates to CAMP (i.e., ~ 200 Ma). The South Georgia Rifts are known to be capped by the magmatic complexes from this event (e.g., McBride, 1991; Marzen et al., 2020). The potential continuation of the South Georgia Rift system - the Apalachicola Basin (labeled “AB” in **Figures 5A** and **5D**) requires dense and highly magnetic rocks to explain the observed magnetic anomalies (Liu et al., 2019) that we interpret as CAMP, thus being emplaced around 200 Ma. We expand this interpretation to other mapped magmatic complexes mapped from seismic and potential fields, particularly to SDRs (**Figures 5** and **6**) as being added during the CAMP magmatic event along both the eastern margin of Florida and the western Yucatan. None of the other seismic lines show this volume of volcanic activity, therefore, it is unlikely that these two inner SDR basalt basins formed adjacent to any of the other portions of the rifted basin. Therefore, these areas were adjacent to each other around 200 Ma (**Figure 7B**).

Paleogeographically, in order to have the two inner SDRs adjacent to each other, the Yucatan block needs to rotate dramatically counterclockwise in approximately 5 million years and the rifting needs to progress from scattered continental rifting to focused rifting resulting in the stretched and intruded continental crust as we have modeled in **Figure 7B**. While this may appear to be too dramatic for these slow-moving continental blocks, there is other evidence for a major tectonic upheaval. The CAMP dikes in southeastern

North America were initially injected oriented in an NW - SE direction parallel to the inner SDRs around 200 Ma (e.g., Nomade et al. 2007, Beutel, 2009; Marzen et al, 2020). Both the ~200 Ma dikes and SDRs indicate a change in the extension direction from NW-SE tensional stress that formed the NE-SW trending rifts to NNE-SSW tensional stress that formed the NNW-SSE trending dikes and inner SDRs, all of which make a major plate motion change reasonable. Because the South Georgia Rift ceases to extend (i.e., McBride, 1991), all southward motion of Florida is modeled as ceasing at ~ 205 Ma. Tectonically, the rapid motion change of both the stress field and the motion of the Yucatan is likely caused by the separation of Florida from South America and the Yucatan. Prior to ~ 205 Ma, Florida and South America were still connected as were Florida and Africa, this combined motion created the NE-SW trending extensional basins. However, when South America was separated from Florida by oceanic crust (**Figure 7B**), it ceased having any influence on Florida, thus changing the internal stress field of the Florida block. Because South America was still attached to the Yucatan, it continued to influence the motion of the Yucatan, perhaps resulting in the rotation of the Yucatan which created a stress field almost 90 degrees from the original.

- **Early - Middle Jurassic (195 Ma-165 Ma)**

Between ~195 Ma and ~165 Ma, our plate reconstruction (**Figures 7E** and **7F**) is guided by the existence of pre-salt basins that developed in the east (what is now the northeastern GoM and the western Yucatan margin) but were not formed in the west (what is now the Texas margin and the southern Yucatan/Chiapas block). We explain this with the post-magmatic subsidence of the crust in the east that did not occur in the west. The western thickened crust formed during the Ouachita orogeny was not extended in the Triassic in contrast to the crust in the east (**Figure 7A**). In the west, only the lower crust is intruded (**Figures 5B** and **5C**), while in the east there are upper, middle, and lower crustal mafic intrusions (**Figures 5D**, **5E**, **5I**, and **5K**). The volume of intrusions, thinner crust, and proximity to excessive mafic volcanism in South Florida around 200 Ma (**Figure 1A**) suggest that the eastern continental crust was significantly hotter than the western one. As the magmatism in the east ceased by around 195 Ma, the eastern continental crust began subsiding and accumulated a large body of sediments prior to deposition of salt at 169 Ma. In contrast, the thicker and more buoyant western GOM crust remain elevated and failed to accumulate a significant pre-salt sedimentary section (**Figures 7D** and **7E**). This is consistent with observations of Dickinson et al. (2010) in central Texas suggesting a local uplift of that region at late Triassic - early Jurassic, as well as with observations of Ewing and Galloway (2019) noting a general lack of early Jurassic deposits in the northwestern GoM.

Our reconstruction suggests that the rate of southward motion of the Yucatan relative to North America increases as the rotation of the Yucatan, seen between 205 and 195 Ma, ceased. This is likely due to the development of thinned transitional crust and the increased rate of motion of South America. North America's effect on the Yucatan is hampered by a transitional crust that doesn't transmit stress well, but likely helps to guide the relative motion that is more strongly affected by South America (**Figure 7C**). When oceanic crust formation begins is perhaps best identified by the sudden increase in rate of relative motion of continents to North America. Around 200 Ma it is clear that South America is no-longer completely tied to North America and that oceanic crust has likely developed between the Florida/Suwanee block and South America (compare **Figure 7A** to **Figure 7B**). We also see a dramatic increase in the rate of motion of Africa relative to North America at 195 Ma, suggesting that the two are now separated by a weak zone and some oceanic crust (compare **Figure 7B** and **Figure 7C**). These relative motions and relationships between the plates continue until around 165 Ma. By that time, the salt is deposited throughout

the entire Gulf of Mexico (Pindell et al., 2020). In the east, the salt is deposited on thick sedimentary sequences (butter-yellow in **Figures 7D, 7E, 7F**), while in the west, deposition occurs on the transitional crust that is now subsiding as it stretches (**Figure 7D** lighter-blue). Africa no longer has any influence on the Gulf of Mexico area.

- **Late Jurassic oceanic Phase 1 (165-152 Ma)**

Between 165 and 152 million years ago, our reconstruction is based on the interaction of the Yucatan with the plates around it and the seafloor spreading which initiates at ~165 Ma in our model (loosely constrained by the age of ~ 160 Ma determined by Snedden et al., 2014). Specifically, the interaction of the southwestern corner of the Yucatan and the Maracaibo block (**Figure 7E**), which, along with other subduction zones in that area, causes the Yucatan block to begin rotating. The rate of rotation is limited by the ongoing connection between the Yucatan and the North American continental crust in the center of the basin (the still connected stretched continental crust with evidence of post-salt exhumation of lower continental crust, **Figure 5F**) and the thin, ultra-slow spreading oceanic crust in the east and the west (as seen in **Figure 5**). The sudden acceleration of South America during this interval suggests that the connection between the Yucatan and South America has weakened to the point when South America and the Yucatan no longer influence each other. Instead, the Yucatan appears to be guided by the motion of the Mexican terrains that will make up Mexico and parts of Central America. Around 165 Ma, the transitional crust along the northeast and northwest corners of the Yucatan finally thins enough to start oceanic spreading (**Figure 7F**). However, the relative motion to North America remains very slow, so the produced oceanic crust, as seen in **Figure 5**, is magma starved and very thin. The rate of spreading is likely slowed by the oblique spreading orientation (**Figure 7F**) and continued continental connection between North America and the Yucatan. While highly oblique back-arc basins have been proposed to account for the motion of the Yucatan (Stern and Dickinson, 2010), the rotation and motion can be explained by the interaction of the Yucatan with the Southeast moving terranes of Mexico (**Figures 7E and 7F**).

- **Late Jurassic - Early cretaceous oceanic Phase 2 (152-135 Ma)**

Between 152 and 135 million years ago, the reconstruction of the motion of the Yucatan was constrained mostly by the Phase 2 oceanic spreading centers and transform faults (**Figure 6**). However, the different rate of rotation is modeled with respect to Phase 1 because of the change in the connection between the Yucatan and North America (compare the northern boundary of the Yucatan in **Figures 7F and 7G**). The last connection of continental crust between North America and the Yucatan is broken by the onset of a slow-spreading ridge in the center of the basin around 152 Ma. An apparent increase in the rate of rotation (**Figure 7G, Table 2**) corresponds to an increase in the spreading rate and in increased magmatic supply; as is seen in **Figure 5**, oceanic crust is now thicker and two-layered. By approximately 135 Ma (**Figure 7H**), the subduction zone between the Yucatan and the Mexican terranes has closed, and the Yucatan now moves as part of the North American plate. This causes the mid-ocean ridge in the Gulf of Mexico to cease spreading and all the relative motion between North America and South America rearranges to the spreading ridge in the Caribbean.

Tectonic Reconstruction Summary

~230 - ~205 Ma Yucatan is emplaced into North America, rotated so the present day NW coast is parallel to the western edge of Florida. Slow continental stretching as North America moves to the NW away from the rest of Pangea results in NE trending rift basins. (**Figure 7A**).

~205-195 Ma Yucatan and Florida terranes separate, Yucatan rotates ~30 degrees counterclockwise, and inner SDRs form as part of the Central Atlantic Magmatic Province. Yucatan is still tectonically connected to North America and South America; Florida is now permanently attached to North America. (**Figures 7B-7C**).

~195-~165 Ma General south-southeast motion of the Yucatan block continues to be guided by the motion of North America and South America. Transitional crust forms around the Gulf of Mexico, but thick sedimentary sequences only form where excess magmatism during CAMP cooled and resulted in their subsidence. A thick layer of salt is deposited between 170 Ma and 165 Ma (Pindell et al., 2020). (**Figure 7D**).

~165-~150 Ma A subduction zone forms along the southwest margin of the Yucatan dipping under the Maracaibo block causing the Yucatan to begin to rotate. Ultra-slow spreading crust is formed along the northwestern and northeastern margins of the Yucatan, but transitional crust still connects the Yucatan and North America in the ‘center of the basin (**Figures 7E-7F**).

~150 Ma Southwest subduction continues under what will become Mexico. Transitional crust no-longer connects North America and the Yucatan resulting in an increase in rotation speed, a new ridge, and the formation of slow-spreading oceanic crust. (**Figure 7F**).

~135 Ma Yucatan docks with Mexico and all tectonic motion in the Gulf of Mexico ceases. (**Figure 7H**).

6. Conclusions

Integration of multiple geophysical datasets with geological observations allowed us to derive strong constraints for tectonic reconstruction of the Gulf of Mexico, such as Triassic rifts, CAMP-related magmatic complexes, Early to Middle Jurassic sedimentary basins developed prior to deposition of salt, and two distinct oceanic spreading episodes in Late Jurassic through Early Cretaceous. Our tectonic reconstruction allows us to draw the following conclusions:

1. The magmatic regime varied during the basin formation from the CAMP magmatic event to amagmatic post-salt rifting that resulted in the exhumation of the lower continental crust.
2. The number of matching geological observations, namely SDRs, pre-salt basin, and outer troughs underlined by an exhumed lower crust, suggest that the northeastern GoM and the western Yucatan are conjugate margins.
3. Rotation of Yucatan between 205 Ma and 195 Ma explains the termination of the South Georgia Rift system and the emplacement of NW-SE trending dikes on top of NE-SW trending rift basins.
4. Our reconstruction suggests that the ~170 Ma rotation of the Yucatan initiated with the formation of a subduction zone between the Yucatan and the Maracaibo block.

5. Ridge reorganization occurred during the formation of oceanic crust that resulted in two sets of extinct spreading centers. The older ultra-slow spreading (~165 -152 Ma) produced thin and uniform crust, while the younger slow-spreading episode (~152 - 135 Ma) resulted in a thicker and layered crust with NW-SE trending spreading centers.

The use of geologic features identified using geophysical methods, combined with the analysis of how the Yucatan is interacting with all surrounding plates at any given time lends robustness to our model.

7. Acknowledgments

The authors are extremely grateful to TGS, and particularly to Jim Howell for allowing us to use proprietary seismic data shown in **Figure 2** for our analysis. Many thanks go to Jerry Bartholomew and another anonymous reviewer for thorough reviews and constructive criticism that improved the paper.

8. Tables

Table 1. The list of tectonic constraints used for each reconstruction period

Observation	Interpretation	Timing	Implication	Constraint	Reconstruction
Triassic rifts evident in potential field data (Figure 3)	Stretching of Florida and Yucatan terrains attached to North America	~ 230 - 205 Ma based on dated Eagle Mills and South Georgia Rifts	Both Florida and Yucatan are welded to North America	The rifts must be aligned when reconstructed	Figure 7A
Magmatic addition (SDRs, igneous intrusions in the lower and middle crust, Figures 2, 5 and 6)	Evidence of magmatic activity during continental rifting stage	SDRs ~ 190 Ma (per DSDP well 535A), but interpreted as CAMP related event (~200 Ma)	Magmatic burst during the continental rifting	The SDRs on the Yucatan block and on the North American margin should be near each other once reconstructed	Figure 7B
Pre-salt sedimentary basins on transitional crust in the eastern and in the southern GoM (Figures 5 and 6)	The syn-rift sediments before the deposition of salt at ~ 169 Ma (Figure 4)	From ~ 190 to ~ 169 Ma, most likely deposited in the sag formed due to cooling at the end of the SDR magmatism	Local subsidence in the east to accumulate thick sediments. Local uplift in the west as no pre-salt section developed.	Pre-salt basins should be proximal once restored	Figures 7C-7E
Outer Trough (Figures 2 and 5A) and zone of significant thickening of Jurassic strata in the Northern Yucatan	Evidence of uncontrolled flow of salt with the Jurassic overburden (Hudec and Norton, 2019)	Post-salt continental stretching (~ 169 – 165 Ma)	Interpreted as exhumation of lower continental crust suggesting no magmatism immediately before oceanic spreading	Initial oceanic spreading likely to be ultra-slow	Figure 7F
Phase 1 of oceanic spreading producing thin (~ 5 km) and uniform oceanic crust (Figures 2, 5 and 6)	Ultra-slow spreading (estimated 0.9 cm/yr, Filina et al., 2020)	~ 165 – ~ 152 Ma Ridge reorganization at ~ 152 Ma	Rotation of the Yucatan around the nearby pole produces Phase 1 spreading centers, low availability of magmatic material	The Phase 1 crust from Yucatan and North America should be adjacent during reconstruction	Figure 7F

Phase 2 of oceanic spreading resulting in thicker (up to 9 km) and layered crust (Figures 2, 5 and 6)	Slow spreading (estimated 1.1 cm/yr, Filina et al., 2020)	~ 152 – ~ 135 Ma Timing is loosely constrained by Snedden et al., 2014.	Final separation of Yucatan from North America allows southward migration of the Yucatan block; Increase in magma supply	All oceanic crust should be formed by ~ 135 Ma	Figures 7G-7H
--	---	--	--	--	----------------------

Table 2. Kinematic parameters determined from tectonic reconstruction in **Figure 7**. All poles are versus North America.

Time (Ma)	Latitude	Longitude	Angle
220	24.3332	-85.7972	-94.2209
205	24.0279	-85.7491	-93.7897
200	23.8349	-85.4426	-68.5622
162	22.1944	-87.271	-60.8887
151	22.2691	-87.3824	-44.8

9. Figure Captions

Figure 1: (A) The first vertical derivative of the gravity field from Sandwell et al. (2014), the greyscale color scheme is as in the original publication and means to highlight geological structures. Of particular interest are the apparent NW-SE trending lineaments in the middle of the Gulf of Mexico basin that are interpreted as segments of extinct spreading centers offset by transform faults. Pink polygons outline the extents of salt basins from Snedden and Galloway (2019). Red arrows point on the Paleozoic Ouachita-Marathon orogenic belt related to the assembly of Pangea. The white rectangle shows the extent of the zoomed section shown in panel (B). NA= North America, YUC= Yucatan crustal block, FL= Florida crustal block. (B) Locations of published Ocean-Continent boundaries (OCB) for the Gulf of Mexico plotted with different colors. The circles are poles of rotation from different publications. The two of the published tectonic models are shown with solid and dashed lines as they include tectonic boundaries for two stages – the initial breakup (dashed line) and the Yucatan rotational phase (solid line of the same color). The poles of rotation from this study (larger red circles) are given in **Table 2**.

Figure 2. Seismic cross-sections (data courtesy of TGS) illustrating various tectonic zones and geological structures in the Gulf of Mexico (A) a regional seismic line from the northwestern GoM to the Yucatan margin from the recent GIGANTE survey (from Filina et al., in review). Blue (5 km long) and red (7.5 km) vertical arrows mark interpreted oceanic crust produced in Phase 1 (~ 165 -152 Ma, ultra-slow) and Phase 2 (~ 152 - 135 Ma, slow) oceanic spreading respectively. YSC = Young spreading center, BAHA refers to the BAHA high outlined by Hudec et al. (2020) shown in **Figure 5A**. (B) a regional cross-section through the eastern GoM (from Snedden et al., 2014 and Lin et al., 2019). Note apparent variations in the crustal thickness in the oceanic domain and challenges of the subsalt seismic image in the continental regions. OSC - Old Spreading Center (to be compared with **Figure 5**).

Figure 3. (A) Residual gravity field (original data from Sandwell et al., 2014 corrected for water and the upper mantle gravity signals, see text for details). The dashed black line follows the sharp edge of the carbonate platforms that is apparent in gravity data. (1) marks the gravity low over the thick salt structure known as “salt wall” in the northwestern GoM, (2) label the characteristic gravity and magnetic lows and highs interpreted as Triassic rifts in the northeastern GoM and the Yucatan margin; these structures are aligned in the tectonic restoration for 220 Ma in **Figure 7A**. (3) point on pronounced gravity lows and magnetic highs associated with the Phase 2 extinct spreading center (mapped with black segments in **Figure 5A**); (B) Reduced to Pole magnetics from Minguez et al. (2020) in the center and from Meyer et al. (2017) near the shoreline. (4) marks the magnetic anomalies responsible for interpreted SDR complexes. (C) Example of integrated geophysical modeling for the profile through the western GoM; the location is shown as a black line in maps (A) and (B). The top panels show observed and computed gravity and magnetic fields. The model shown in the bottom panel uses the seismic reflection data from Pindell et al. (2020) to constrain multiple subsurface layers. See the physical properties of each subsurface layer in the legend for **Figure 5**. UCC = upper continental crust, LCC = lower continental crust

Figure 4: Simplified geologic time chart listing the major tectonic events related to the opening of the Gulf of Mexico.

Figure 5. (A) Key tectonic structures mentioned in the literature and interpreted in our study (see text for details and references). The thin black lines show the cross-sections developed from the integration of seismic reflection, refraction, gravity, and magnetic data. (B) the model along GUMBO1 (Van Avendonk

et al., 2015; Filina, 2019), (C) GUMBO2 (Eddy et al., 2018; Filina, 2019), (D) GUMBO3 (Eddy et al., 2014; Liu et al., 2019), (E) GUMBO4 (Christeson et al., 2014; Liu and Filina, 2018), (F-H) lines L1 through L3 from William-Rojas et al. (2012) modeled by Filina and Hartford (2021), (I) modified model of Filina (2020) along a seismic line shown in **Figure 2B**, (J) interpreted seismic profile from TGS GIGANTE survey shown in **Figure 2A**, and (K) an interpretation for the seismic line of Horn et al. (2017; not shown here), please note that the line is split into two segments to keep the same scale as other lines. The same markers as in **Figure 2** are used to show locations of interpreted tectonic features: OCB (blue), pre-salt basin (green), magmatic complexes (referred to as SDR in literature) are brown, and pseudofaults marking the boundary between old and new oceanic crustal zones are marked with yellow circles. OC = oceanic crust

Figure 6: Filtered residual potential fields data (A) residual Bouguer gravity; the dashed black line marks the shelf break that is associated with a sharp change in bathymetry that is evident in filtered gravity data, (B) residual RTP magnetic, (C, D) show interpreted tectonic zones. The same symbology is used as in **Figures 2 and 5.**

Figure 7. Tectonic reconstructions of the Gulf of Mexico using GPlates version 2.2 and modifying global plate motions based on Mueller et. al (2019). Each plate, microplate, or geologic structure is assigned its own color by GPlates; arrows generated by GPlates indicate the relative velocity of that point on a plate to a fixed North American plate. If no arrows are present that plate is not moving relative to North America. Each reconstruction has a slightly different scale for the arrows as indicated in each figure.

(A) 220 Ma reconstruction of the Gulf of Mexico. Reconstruction is based on the alignment of the Triassic rifts in the Yucatan and Florida (Pindell and Keenan, 2009; labeled as “2” in **Figure 3**), the deformation in continental rocks, and the pre-existing structures created during the rifting of Rodinia (Thomas, 2006; shown as thin white lines in **Figure 7A**). Reconstruction shows a snapshot of the plates positions and motions during the 230 Ma-205 Ma time period. To account for the continental stretching of the Yucatan and Florida between 230 Ma and 205 Ma, they were emplaced in North America and moved south the approximate amount they were stretched. The South Georgia Rift was also formed during this time and the approximate location of the faults is taken from Hefner (2013).

(B) 200 Ma reconstruction of the Gulf of Mexico based on the inner SDRs identified in **Figure 5A** shown as dark blue regions. CAMP volcanism from this time period is indicated via the NW trending CAMP dikes seen throughout the SE United States. White lines show postulated plate boundaries, boxes indicate normal faulting/extension. Note that no plate boundary is assumed between SA and the Yucatan.

(C) 195 Ma reconstructions based on location of the seaward dipping reflectors (SDRs) and the development of transitional crust. When compared to the motion at 200 Ma, South America has changed its relative motion by almost 90 degrees. Along with the intrusion of the CAMP mafics, this relative motion change may actually have facilitated the rotation of the Yucatan between 205 Ma and 195 Ma

(D) 170 Ma reconstruction of the incipient Gulf of Mexico. Transitional crust has been almost entirely created at this time and has two different signatures. The butter-yellow areas near the Yucatan and in the northeastern Gulf of Mexico are transitional crust that has sunk considerably as the magmatism from CAMP cools resulting in deposition of thick sedimentary sequences prior to 170 Ma (**Figures 5 and 6**). The transitional crust in the northwestern Gulf of Mexico (lighter blue) does not have any thick sedimentary sequences and appears to have been relatively high standing prior to this time period. Note the beginning

of contact between the Maracaibo (MA) block and the Yucatan, which has been determined to be a subduction zone.

(E) 163 Ma reconstruction of the incipient Gulf of Mexico. Due to collision with the Maracaibo block and the initiation of subduction, the Yucatan block is now rotating rapidly; all transitional crust is now formed and ultra-slow spreading will commence. Thick salt deposits now cover all the basin (since ~ 169 Ma, Pindell et al., 2020; **Figure 4**).

(F) 153 MA reconstruction of the incipient Gulf of Mexico basin. New features include the thin, ultra-slow spreading crust identified in **Figure 5**, shown as the present day filtered residual satellite gravity of those regions (from **Figure 6A**). Note that the pole of rotation relative to North America for the Yucatan is the same as it was at 163 Ma and that the Yucatan is still attached to North America via transitional crust between the two ultra-slow spreading centers. The black double headed arrows indicate the extension direction across the plate boundary.

(G) 143 Ma reconstruction of the forming Gulf of Mexico basin. The Yucatan has now completely broken free from North America which has caused an increase in the rate of rotation, resulting in the thicker and layered crust seen in **Figure 5** and the formation of a new spreading ridge (all oceanic crust is shown via the residual gravity from **Figure 6A**. Possible ridges (thick black lines) and transforms (dashed lines) have been noted. The pseudofaults generated during propagation of the new ridge are shown as yellow lines as in **Figure 5A**.

(H) 134 Ma reconstruction of the Gulf of Mexico basin. The Yucatan has now stopped moving after docking with southern Mexico. The oceanic domain consists of two different crustal zones separated by a pseudofault (symbolology as in **Figure 5A**). The older oceanic crust is not layered and is thin, while the younger crust is the result of faster spreading and is thicker and at least two layers as shown in **Figures 2** and **5**.

10. References

- Ball, M.M., Martin, R.G., Foote, R.Q. and Applegate, A.V., 1988. Structure and stratigraphy of the western Florida shelf; Part I, Multichannel reflection seismic data (No. 88-439). US Geological Survey.
- Bankey, V., Cuevas, A., Daniels, D., Finn, C.A., Hernandez, I., Hill, P., Kucks, R., Miles, W., Pilkington, M., Roberts, C. and Roest, W., 2002. Digital data grids for the magnetic anomaly map of North America (No. 2002-414).
- Barboza-Gudiño, J.R., Zavala-Monsiváis, A., Venegas-Rodríguez, G. and Barajas-Nigoche, L.D., 2010. Late Triassic stratigraphy and facies from northeastern Mexico: Tectonic setting and provenance. *Geosphere*, 6(5), pp.621-640.
- Beutel, E.K., 2009. Magmatic rifting of Pangaea linked to onset of South American plate motion. *Tectonophysics*, 468(1-4), pp.149-157.
- Bird, D.E., Burke, K., Hall, S.A. and Casey, J.F., 2005. Gulf of Mexico tectonic history: Hotspot tracks, crustal boundaries, and early salt distribution. *AAPG bulletin*, 89(3), pp.311-328.

Christeson, G.L., Van Avendonk, H.J.A., Norton, I.O., Snedden, J.W., Eddy, D.R., Karner, G.D. and Johnson, C.A., 2014. Deep crustal structure in the eastern Gulf of Mexico. *Journal of Geophysical Research: Solid Earth*, 119(9), pp.6782-6801.

Coombs, H., Kerr, A., Pindell, J., Buchs, D., Weber, B. and Solari, L., 2019. Petrogenesis of the crystalline basement along the western Gulf of Mexico: Postcollisional magmatism during the formation of Pangea. Southern and central Mexico: basement framework, tectonic evolution, and provenance of Mesozoic-Cenozoic basins. *GSA Special Paper*.

Corti, G., 2012. Evolution and characteristics of continental rifting: Analog modeling-inspired view and comparison with examples from the East African Rift System. *Tectonophysics*, 522, pp.1-33.

Curry, M.A., Peel, F.J., Hudec, M.R. and Norton, I.O., 2018. Extensional models for the development of passive-margin salt basins, with application to the Gulf of Mexico. *Basin Research*, 30(6), pp.1180-1199.

Deighton, I.C., Winter, F. and Chisari, D., 2017. Recent high-resolution seismic, magnetic and gravity data throws new light on the early development of the Gulf of Mexico. In *AAPG Annual Meeting Abstracts*, Houston.

Dickinson, W.R., Gehrels, G.E. and Stern, R.J., 2010. Late Triassic Texas uplift preceding Jurassic opening of the Gulf of Mexico: Evidence from U-Pb ages of detrital zircons. *Geosphere*, 6(5), pp.641-662.

Dobson, L.M. and Buffler, R.T., 1991. Basement rocks and structure, northeast Gulf of Mexico.

Eddy, D.R., Van Avendonk, H.J., Christeson, G.L., Norton, I.O., Karner, G.D., Johnson, C.A. and Snedden, J.W., 2014. Deep crustal structure of the northeastern Gulf of Mexico: Implications for rift evolution and seafloor spreading. *Journal of Geophysical Research: Solid Earth*, 119(9), pp.6802-6822.

Eddy, D.R., Van Avendonk, H.J., Christeson, G.L. and Norton, I.O., 2018. Structure and origin of the rifted margin of the northern Gulf of Mexico. *Geosphere*, 14(4), pp.1804-1817

Erlich, R.N. and Pindell, J., 2020. Crustal origin of the West Florida Terrane, and detrital zircon provenance and development of accommodation during initial rifting of the southeastern Gulf of Mexico and western Bahamas. *Geological Society, London, Special Publications*, 504.

Escalona, A., I. O. Norton, L. A. Lawver, and L. Gahagan, in press, Quantitative plate tectonic reconstructions of the Caribbean region from Jurassic to present, in C. Bartolini, ed., Eastern Caribbean–northeastern South American boundary: Tectonic evolution, basin architecture, and petroleum systems: *AAPG Memoir 123*.

Ewing, J., Antoine, J. and Ewing, M., 1960. Geophysical measurements in the western Caribbean Sea and in the Gulf of Mexico. *Journal of Geophysical Research*, 65(12), pp.4087-4126.

Fiduk, J.C., Weimer, P., Trudgill, B.D., Rowan, M.G., Gale, P.E., Phair, R.L., Korn, B.E., Roberts, G.R., Gafford, W.T., Lowe, R.S. and Queffelec, T.A., 1999. The Perdido fold belt, northwestern deep Gulf of Mexico, part 2: seismic stratigraphy and petroleum systems. *AAPG bulletin*, 83(4), pp.578-612.

Filina, I., Delebo, N., Mohapatra, G., Coble, C., Harris, G., Layman, J., Strickler, M. and Blangy, J.P., 2015. Integration of seismic and gravity data—A case study from the western Gulf of Mexico. *Interpretation*, 3(4), pp. SAC99-SAC106.

- Filina, I., 2019. Crustal architecture of the northwestern and central Gulf of Mexico from integrated geophysical analysis. *Interpretation*, 7(4), pp. T899-T910.
- Filina, I., Liu, M. and Beutel, E., 2020. Evidence of ridge propagation in the eastern Gulf of Mexico from integrated analysis of potential fields and seismic data. *Tectonophysics*, 775, p.228307.
- Filina, I., 2020. Ridge propagation in the eastern Gulf of Mexico from integrated geophysical modeling. In SEG Technical Program Expanded Abstracts 2020 (pp. 915-919). Society of Exploration Geophysicists.
- Filina, I. and Hartford, L., 2021. Subsurface structures along western Yucatan from integrated geophysical analysis. *Marine and Petroleum Geology*, 127, p.104964.
- Filina, I., Austin, J.A., Doré, A.G., Johnson, E.A., Minguez, D.A., Norton, I.O., Snedden, J. and Stern, R.J., Opening of the Gulf of Mexico: what we know, what questions remain, and how we might answer them, in review in *Tectonophysics*
- Frizon de Lamotte, D., Fourdan, B., Leleu, S., Leparmenier, F. and de Clarens, P., 2015. Style of rifting and the stages of Pangea breakup. *Tectonics*, 34(5), pp.1009-1029.
- Galloway, W. E., 2008, Depositional evolution of the Gulf of Mexico sedimentary basin, in A. D. Miall, *Sedimentary basins of the world*, Elsevier Science, v. 5, p. 505-549.
- Godínez-Urban, A., Lawton, T.F., Molina -Garza, R.S., Iriondo, A., Weber, B. and López-Martínez, M., 2011a. Jurassic volcanic and sedimentary rocks of the La Silla and Todos Santos Formations, Chiapas: Record of Nazas arc magmatism and rift-basin formation prior to opening of the Gulf of Mexico. *Geosphere*, 7(1), pp.121-144.
- Godínez-Urban, A., Molina-Garza, R.S., Geissman, J.W. and Wawrzyniec, T., 2011b. Paleomagnetism of the Todos Santos and La Silla Formations, Chiapas: implications for the opening of the Gulf of Mexico. *Geosphere*, 7(1), pp.145-158.
- Gottfried, D., Annell, C.S. and Byerly, G.S., 1983. Geochemistry and tectonic significance of subsurface basalts from Charleston, South Carolina: Clubhouse Crossroads test holes# 2 and# 3. US Geol Survey Prof Paper, 1313, pp.A1-A10.
- Guan, H., Geoffroy, L., Gernigon, L., Chauvet, F., Grigne, C. and Werner, P., 2019. Magmatic ocean-continent transitions. *Marine and Petroleum Geology*, 104, pp.438-450.
- Hall, S.A. and Najmuddin, I.J., 1994. Constraints on the tectonic development of the eastern Gulf of Mexico provided by magnetic anomaly data. *Journal of Geophysical Research: Solid Earth*, 99(B4), pp.7161-7175.
- Heffner, D.M., Knapp, J.H., Akintunde, O.M. and Knapp, C.C., 2012. Preserved extent of Jurassic flood basalt in the South Georgia Rift: A new interpretation of the J horizon. *Geology*, 40(2), pp.167-170.
- Heffner, D.M., 2013. Tectonics of the South Georgia Rift. (Thesis)
- Hilterman, F., 1998, Rock property framework for comprehending deep – water seismic response
- 14th Annual Gulf Coast Technical Meeting, SEG1998

- Hinz, K., 1981. A hypothesis on terrestrial catastrophes: Wedges of very thick oceanward dipping layers beneath passive margins. *Geologisches Jahrbuch*, ser. E, v. 22, p. 5-28
- Horn, B., Hartwig, A., Faw, J., Novianti, I., Goswami, A. and McGrail, A., 2017. Refining exploration opportunities in Mexico. *GEOExPro*, 14, pp.64-69.
- Hudec, M.R., Norton, I.O., Jackson, M.P. and Peel, F.J., 2013. Jurassic evolution of the Gulf of Mexico salt basin, *AAPG Bulletin*, 97(10), pp.1683-1710.
- Hudec, M.R. and Norton, I.O., 2019. Upper Jurassic structure and evolution of the Yucatán and Campeche subbasins, southern Gulf of Mexico. *AAPG Bulletin*, 103(5), pp.1133-1151.
- Hudec, M.R., Dooley, T.P., Peel, F.J. and Soto, J.I., 2020. Controls on the evolution of passive-margin salt basins: Structure and evolution of the Salina del Bravo region, northeastern Mexico. *AAPG Bulletin*, 132(5-6), pp.997-1012.
- Huerta, A.D. and Harry, D.L., 2012. Wilson cycles, tectonic inheritance, and rifting of the North American Gulf of Mexico continental margin. *Geosphere*, 8(2), pp.374-385.
- Ibrahim, A.K., Carye, J., Latham, G. and Buffler, R.T., 1981. Crustal structure in Gulf of Mexico from OBS refraction and multichannel reflection data. *AAPG Bulletin*, 65(7), pp.1207-1229.
- Imbert, P., Philippe, Y., Post, P.J., Rosen, N.C., Olson, D.L., Palms, S.L., Lyons, K.T. and Newton, G.B., 2005, December. The Mesozoic opening of the Gulf of Mexico: Part 2. Integrating seismic and magnetic data into a general opening model. In *Transactions of the 25th Annual GCSSEPM Research Conference: Petroleum systems of divergent continental margins* (pp. 1151-1189). Tulsa, Okla: SEPM.
- Imbert, P. and Post, P.J., 2005, December. The Mesozoic opening of the Gulf of Mexico: Part 1, Evidence for oceanic accretion during and after salt deposition. In *Transactions of the 25th Annual GCSSEPM Research Conference: Petroleum systems of divergent continental margins* (pp. 1119-1150).
- Keller, G.R., Pulliam, J., Gurrola, H., Mickus, K., 2016. Extended Abstract: An Overview of the Structure and Tectonic Evolution of the Gulf Coast Region of Texas and Louisiana. *GCAGS Transactions*, 66 (pp 785-788).
- Kneller, E.A. and Johnson, C.A., 2011. Plate kinematics of the Gulf of Mexico based on integrated observations from the Central and South Atlantic.
- Lanphere, M.A. and Gohn, G.S., 1983. $^{40}\text{Ar}/^{39}\text{Ar}$ ages of basalt from Clubhouse Crossroads test hole# 2, near Charleston, South Carolina. US Department of the Interior, Geological Survey.
- Labails, C., Olivet, J.L., Aslanian, D. and Roest, W.R., 2010. An alternative early opening scenario for the Central Atlantic Ocean. *Earth and Planetary Science Letters*, 297(3-4), pp.355-368.
- Laske, G., Masters, G., Ma, Z. and Pasyanos, M., 2013, April. Update on CRUST1. 0—A 1-degree global model of Earth's crust. In *Geophys. Res. Abstr* (Vol. 15, p. 2658).
- Leleu, S., Hartley, A.J., van Oosterhout, C., Kennan, L., Ruckwied, K. and Gerdes, K., 2016. Structural, stratigraphic and sedimentological characterisation of a wide rift system: The Triassic rift system of the Central Atlantic Domain. *Earth-Science Reviews*, 158, pp.89-124.

Lin, P., Bird, D.E. and Mann, P., 2019. Crustal structure of an extinct, late Jurassic-to-earliest Cretaceous spreading center and its adjacent oceanic crust in the eastern Gulf of Mexico. *Marine Geophysical Research*, 40(3), pp.395-418.

Liu, M. and Filina, I., 2018. Potential fields modelling in the northeastern Gulf of Mexico. In AAPG ACE 2018.

Liu, M., Filina, I. and Mann, P., 2019. Crustal structure of Mesozoic rifting in the northeastern Gulf of Mexico from integration of seismic and potential fields data. *Interpretation*, 7(4), pp. T857-T867.

Lundin, E.R. and Doré, A.G., 2017. The Gulf of Mexico and Canada Basin: genetic siblings on either side of North America. *GSA Today*, 27(1), pp.4-11.

MacRae, G. and Watkins, J.S., 1995. Early Mesozoic rift stage half graben formation beneath the DeSoto Canyon salt basin, northeastern Gulf of Mexico. *Journal of Geophysical Research: Solid Earth*, 100(B9), pp.17795-17812.

Martini, M., and F. Ortega-Gutiérrez, 2016, Tectono-stratigraphic evolution of eastern Mexico during the break-up of Pangea: *Earth-Science Reviews*, 183, 38–55, doi:10.1016/j.earscirev.2016.06.013.

Marton, G. and Buffler, R.T., 1994. Jurassic reconstruction of the Gulf of Mexico Basin. *International Geology Review*, 36(6), pp.545-586.

Marzen, R.E., Shillington, D.J., Lizarralde, D., Knapp, J.H., Heffner, D.M., Davis, J.K. and Harder, S.H., 2020. Limited and localized magmatism in the Central Atlantic Magmatic Province. *Nature communications*, 11(1), pp.1-8.

Marzoli, A., Renne, P.R., Piccirillo, E.M., Ernesto, M., Bellieni, G. and De Min, A., 1999. Extensive 200-million-year-old continental flood basalts of the Central Atlantic Magmatic Province. *Science*, 284(5414), pp.616-618.

Marzoli, A., Callegaro, S., Dal Corso, J., Davies, J.H., Chiaradia, M., Youbi, N., Bertrand, H., Reisberg, L., Merle, R. and Jourdan, F., 2018. The Central Atlantic magmatic province (CAMP): A review. *The Late Triassic World*, pp.91-125.

McBride, J.H., 1991. Constraints on the structure and tectonic development of the early Mesozoic South Georgia rift, southeastern United States; seismic reflection data processing and interpretation. *Tectonics*, 10(5), pp.1065-1083.

McHone, J.G., 2003. Volatile emissions from Central Atlantic Magmatic Province basalts: Mass assumptions and environmental consequences. *GEOPHYSICAL MONOGRAPH-AMERICAN GEOPHYSICAL UNION*, 136, pp.241-254.

Meyer, B., Saltus, R. and Chulliat, A., 2017. EMAG2: Earth magnetic anomaly grid (2-arc-minute resolution) version 3. National Centers for Environmental Information, NOAA. Model. doi, 10, p.V5H70CVX.

Minguez, D., Gerald Hensel, E. and Johnson, E.A., 2020. A fresh look at Gulf of Mexico tectonics: Testing rotations and breakup mechanisms from the perspective of seismically constrained potential-fields modeling and plate kinematics. *Interpretation*, 8(4), pp.SS31-SS45

Mjelde, R., Breivik, A.J., Raum, T., Mittelstaedt, E., Ito, G. and Faleide, J.I., 2008. Magmatic and tectonic evolution of the North Atlantic. *Journal of the Geological Society*, 165(1), pp.31-42.

Molina-Garza, R.S., Van Der Voo, R.O.B. and Urrutia-Fucugauchi, J., 1992. Paleomagnetism of the Chiapas Massif, southern Mexico: Evidence for rotation of the Maya Block and implications for the opening of the Gulf of Mexico. *Geological Society of America Bulletin*, 104(9), pp.1156-1168.

Müller, R.D., Zahirovic, S., Williams, S.E., Cannon, J., Seton, M., Bower, D.J., Tetley, M.G., Heine, C., Le Breton, E., Liu, S. and Russell, S.H., 2019. A global plate model including lithospheric deformation along major rifts and orogens since the Triassic. *Tectonics*, 38(6), pp.1884-1907.

Nakamura, Y., Sawyer, D.S., Shaub, F.J., MacKenzie, K. and Oberst, J., 1988. Deep crustal structure of the northwestern Gulf of Mexico.

Netto, A. and Dunbar, J., 2019. 3-D constrained inversion of gravimetric data to map the tectonic terranes of southeastern Laurentia using simulated annealing. *Earth and Planetary Science Letters*, 513, pp.12-19.

Nguyen, L.C. and Mann, P., 2016. Gravity and magnetic constraints on the Jurassic opening of the oceanic Gulf of Mexico and the location and tectonic history of the Western Main transform fault along the eastern continental margin of Mexico. *Interpretation*, 4(1), pp.SC23-SC33.

Nomade, S., Knight, K.B., Beutel, E., Renne, P.R., Verati, C., Féraud, G., Marzoli, A., Youbi, N. and Bertrand, H., 2007. Chronology of the Central Atlantic Magmatic Province: implications for the Central Atlantic rifting processes and the Triassic–Jurassic biotic crisis. *Palaeogeography, Palaeoclimatology, Palaeoecology*, 244(1-4), pp.326-344.

O'Reilly, C., Keay, J., Birch-Hawkins, A., Bate, D. and Halliday, J., 2017. Regional play types in the Mexican Offshore.

Padilla y Sánchez, R.J., 2016. Late Triassic-Late Cretaceous Paleogeography of Mexico and the Gulf of México. Mesozoic of the Gulf Rim and Beyond: New Progress in Science and Exploration of the Gulf of Mexico Basin. GCSSEPM, Houston, TX, 273.

Peace, A., McCaffrey, K., Imber, J., Phethean, J., Nowell, G., Gerdes, K. and Dempsey, E., 2016. An evaluation of Mesozoic rift-related magmatism on the margins of the Labrador Sea: Implications for rifting and passive margin asymmetry. *Geosphere*, 12(6), pp.1701-1724.

Peace, A. L., Phethean, J. J., Franke, D., Foulger, G. R., Schiffer, C., Welford, J. K., ... & Doré, A. G. (2020). A review of Pangaea dispersal and Large Igneous Provinces—In search of a causative mechanism. *Earth-Science Reviews*, 206, 102902.

Pindell, J.L. and Kennan, L., 2009. Tectonic evolution of the Gulf of Mexico, Caribbean and northern South America in the mantle reference frame: an update. *Geological Society, London, Special Publications*, 328(1), pp.1-55.

Pindell, J., Graham, R. and Horn, B., 2014. Rapid outer marginal collapse at the rift to drift transition of passive margin evolution, with a Gulf of Mexico case study. *Basin Research*, 26(6), pp.701-725.

- Pindell, J., Villagómez, D., Molina-Garza, R., Graham, R. and Weber, B., 2020. A revised synthesis of the rift and drift history of the Gulf of Mexico and surrounding regions in the light of improved age dating of the Middle Jurassic salt. Geological Society, London, Special Publications, 504.
- Planke, S., P.A. Symonds, E. Alvestad, J. Skogseid, 2000, Seismic volcanostratigraphy of large-volume basaltic extrusive complexes on rifted margins, *Journal of Geophysical Research: Solid Earth*, 105 (B8) (2000), pp. 19335-19351
- Radovich, B., B. Horn, P. Nuttall, and A. McGrail, 2011, Theonly complete regional perspective: *GeoExPro*,8, 36.
- Ramos, E.L., 1975. Geological summary of the Yucatan Peninsula. In *The Gulf of Mexico and the Caribbean* (pp. 257-282). Springer, Boston, MA.
- Rowan, M.G., 2014. Passive-margin salt basins: Hyperextension, evaporite deposition, and salt tectonics. *Basin Research*, 26(1), pp.154-182.
- Salem, A., Williams, S., Fairhead, D., Smith, R. and Ravat, D., 2008. Interpretation of magnetic data using tilt-angle derivatives. *Geophysics*, 73(1), pp.L1-L10.
- Salvador, A.,1991. Origin and development of the Gulf of Mexico basin. In: Salvador, A. (Ed.), *The Gulf of Mexico Basin. The Geology of North America*, vol. J, pp. 389–444
- Sandwell, D.T., Müller, R.D., Smith, W.H., Garcia, E. and Francis, R., 2014. New global marine gravity model from CryoSat-2 and Jason-1 reveals buried tectonic structure. *Science*, 346(6205), pp.65-67.
- Saunders, M., Geiger, L., Rodriguez, K. and Hargreaves, P., 2016. The Delineation of Pre-Salt License Blocks in the Deep Offshore Campeche-Yucatan Basin.
- Schlager, W., Buffler, R.T., Angstadt, D., Bowdler, J.L., Cotillon, P.H., Dallmeyer, R.D., Halley, R.B., Kinoshita, H., MAGOON III, L.B., McNULTY, C.L. and Patton, J.W., 1984. Deep sea drilling project, leg 77, southeastern Gulf of Mexico. *Geological Society of America Bulletin*, 95(2), pp.226-236.
- Schouten, H. and Klitgord, K.D., 1994. Mechanistic solutions to the opening of the Gulf of Mexico. *Geology*, 22(6), pp.507-510.
- Scott, K.R., Hayes, W.E. and Fietz, R.P., 1961. Geology of the Eagle Mills formation.
- Snadden, J.W., Norton, I.O., Christeson, G.L. and Sanford, J.C., 2014. Interaction of Deepwater Deposition and a Mid-Ocean Spreading Center, Eastern Gulf of Mexico Basin, USA.
- Snadden, J.W. and Galloway, W.E., 2019. *The Gulf of Mexico Sedimentary Basin: Depositional Evolution and Petroleum Applications*. Cambridge University Press.
- Soreghan, G.S. and Soreghan, M.J., 2013. Tracing clastic delivery to the Permian Delaware Basin, USA: Implications for paleogeography and circulation in westernmost equatorial Pangea. *Journal of Sedimentary Research*, 83(9), pp.786-802.
- Soto-Kerans, G.M., Stockli, D.F., Janson, X., Lawton, T.F. and Covault, J.A., 2020. Orogen proximal sedimentation in the Permian foreland basin. *Geosphere*, 16(2), pp.567-593.

- Steier, A. and Mann, P., 2019. Late Mesozoic gravity sliding and Oxfordian hydrocarbon reservoir potential of the northern Yucatan margin. *Marine and Petroleum Geology*, 103, pp.681-701.
- Stern, R.J. and Dickinson, W.R., 2010. The Gulf of Mexico is a Jurassic backarc basin. *Geosphere*, 6(6), pp.739-754.
- Stern, R.J., Anthony, E.Y., Ren, M., Lock, B.E., Norton, I., Kimura, J.I., Miyazaki, T., Hanyu, T., Chang, Q. and Hirahara, Y., 2011. Southern Louisiana salt dome xenoliths: First glimpse of Jurassic (ca. 160 Ma) Gulf of Mexico crust. *Geology*, 39(4), pp.315-318.
- Telford, W.M., Telford, W.M., Geldart, L.P., Sheriff, R.E. and Sheriff, R.E., 1990. *Applied geophysics*. Cambridge university press.
- Thomas, W.A., 2006. Tectonic inheritance at a continental margin. *GSA today*, 16(2), pp.4-11.
- Traverse, A., 1987. Pollen and spores date origin of rift basins from Texas to Nova Scotia as early Late Triassic. *Science*, 236(4807), pp.1469-1472.
- Van Avendonk, H.J., Christeson, G.L., Norton, I.O. and Eddy, D.R., 2015. Continental rifting and sediment infill in the northwestern Gulf of Mexico. *Geology*, 43(7), pp.631-634.
- Williams-Rojas, C.T., Reyes-Tovar, E., Miranda-Peralta, L., Reyna-Martinez, G., Cardenas-Alvarado, A., Maldonado-Villalon, R., Muñoz-Bocanegra, V. and Lora-delaFuente, C., 2011. Hydrocarbon Potential of the Deepwater Portion of the “Salina del Istmo” Province, Southeastern Gulf of Mexico, Mexico.
- Woods, R.D., Salvador, A. and Miles, A.E., 1991. pre-Triassic. The Gulf of Mexico Basin: Boulder, Colorado, Geological Society of America, *Geology of North America*, pp.109-129.
- Wood, G.D. and Benson Jr, D.G., 2000. The North American occurrence of the algal coenobium *plaesiodyctyon*. paleogeographic, paleoecologic, and biostratigraphic importance in the Triassic. *Palynology*, 24(1), pp.9-20.
- Zhao, J., Xiao, L., Gulick, S.P., Morgan, J.V., Kring, D., Fucugauchi, J.U., Schmieder, M., de Graaff, S.J., Wittmann, A., Ross, C.H. and Claeys, P., 2020. Geochemistry, geochronology and petrogenesis of Maya Block granitoids and dykes from the Chicxulub Impact Crater, Gulf of México: Implications for the assembly of Pangea. *Gondwana Research*, 82, pp.128-150.

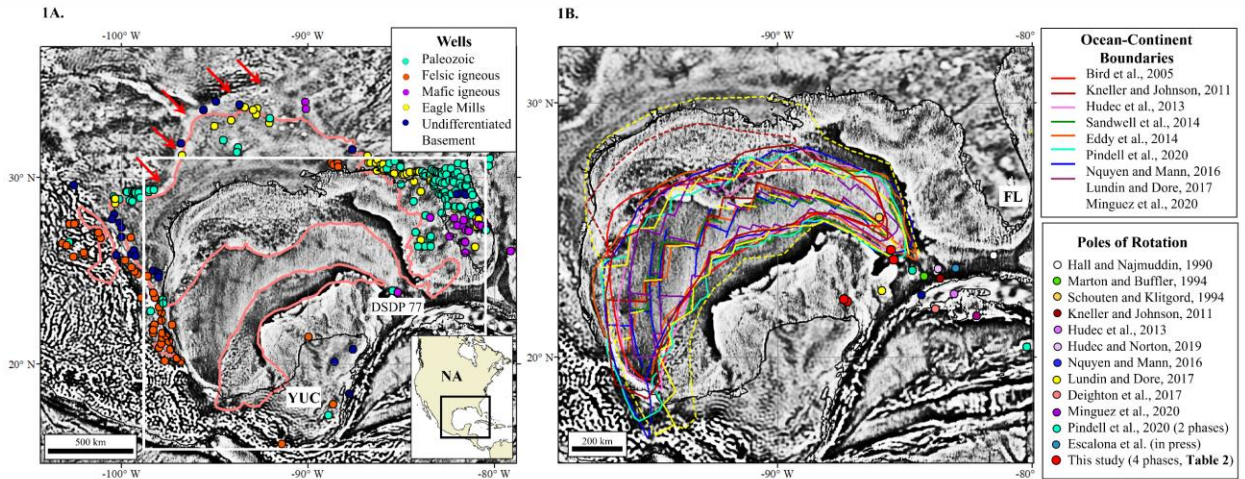


Fig. 2A

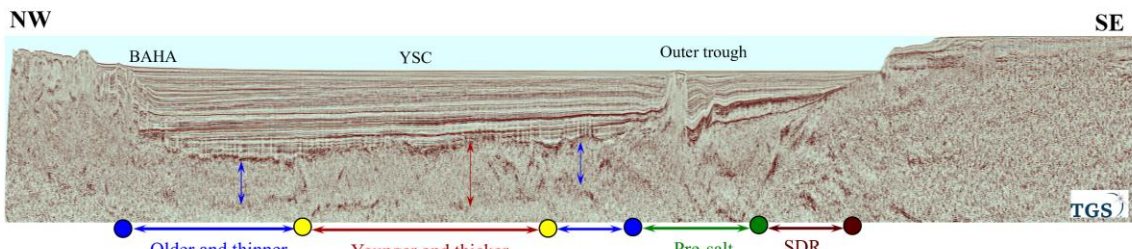
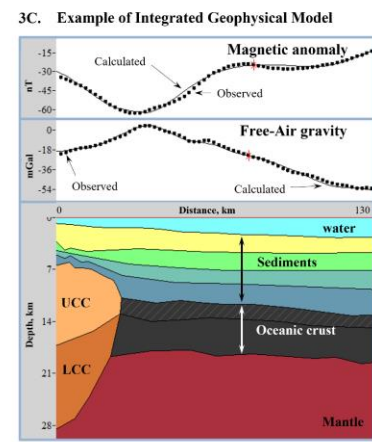
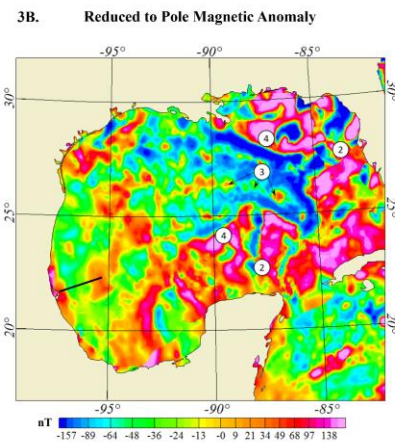
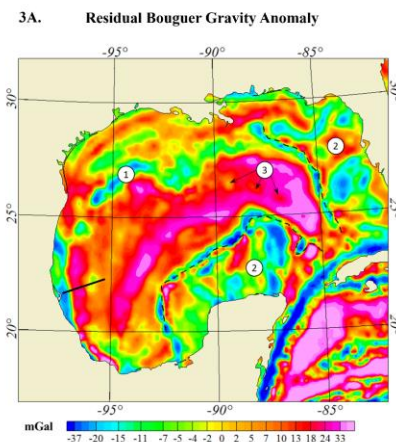
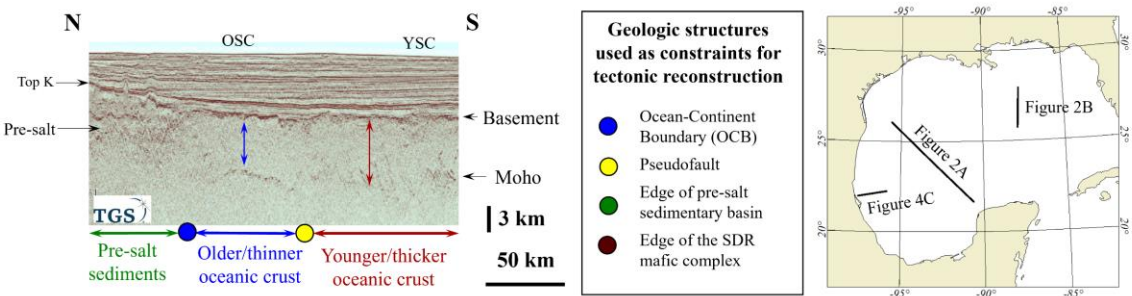


Fig. 2B



PERIOD	EPOCH	AGE	PICKS (Ma)
CRETACEOUS	EARLY	ALBIAN	-113
		APTIAN	-125
		BARREMIAN	-129.4
		HAUTERIVIAN	-132.9
		VALANGINIAN	-139.8
	LATE	BERRIASIAN	-145.0
		TITHONIAN	-152.1
		KIMMERIDGIAN	-157.3
		OXFORDIAN	-163.5
		CALLOVIAN	-166.1
JURASSIC	MIDDLE	BATHONIAN	-168.3
		BAJOCIAN	-170.3
		AALENIAN	-174.1
		TOARCIAN	-182.7
		PLIENSBACHIAN	-190.8
	EARLY	SINEMURIAN	-199.3
		HETTANGIAN	-201.3
		RHAETIAN	-208.5
		NORIAN	-227
		CARNIAN	-237
TRIASSIC	MIDDLE	LADINIAN	-242
		ANISIAN	-247.2
	EARLY	OLENEKIAN	-251.2
		INDIAN	-251.90

Thermal subsidence, formation of passive continental margin, thick carbonate platforms in northeastern and southern parts of the basin

~ **135 Ma** End of oceanic spreading
Phase 2, slow spreading, thick and layered crust

~ **152 Ma** Ridge reorganization
Phase 1, ultra-slow spreading, thin and uniform crust

~ **165 Ma** start of oceanic spreading

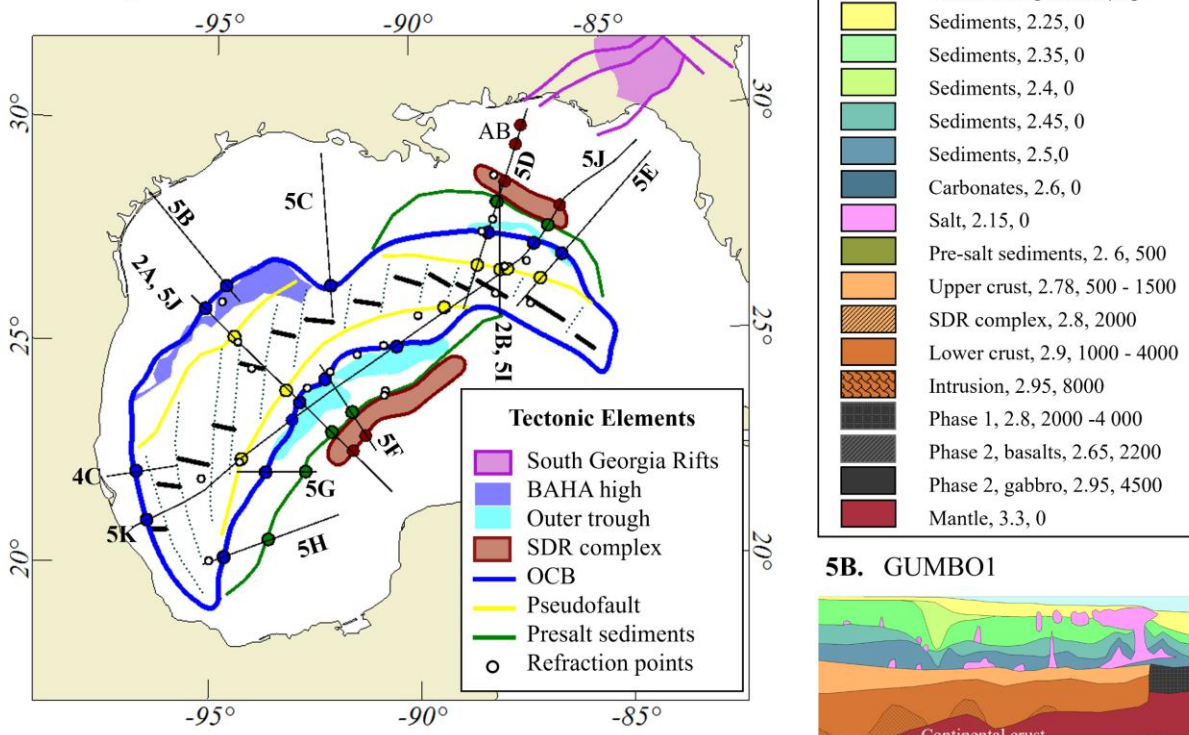
~ **169 Ma deposition of salt**
Pre-salt basins formation, extension and continental thinning is focused in GoM margin

~ **200 Ma CAMP magmatism**

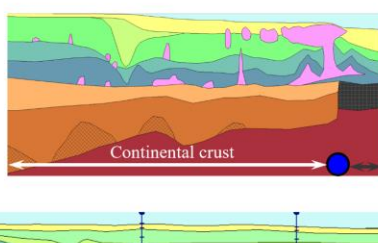
Deposition of Eagle Mills in the northern GoM and its equivalents pre-salt strata in southern GoM

~ **240 extension** in northeastern part of the basin, formation of South Georgia Rifts

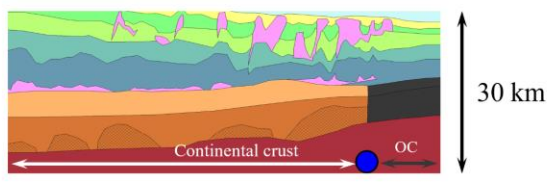
5A. Major tectonic structures in the Gulf of Mexico



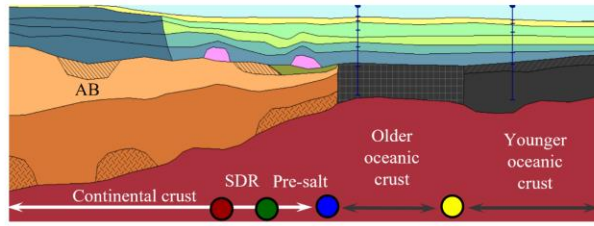
5B. GUMBO1



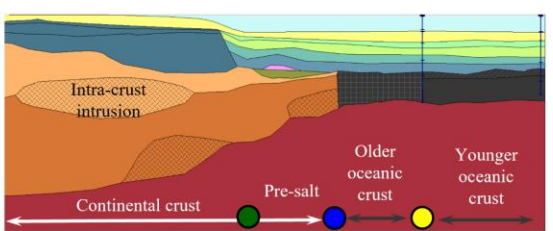
5C. GUMBO2



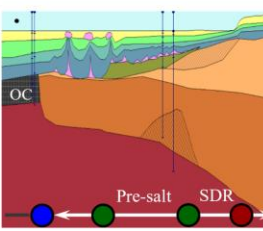
5D. GUMBO3



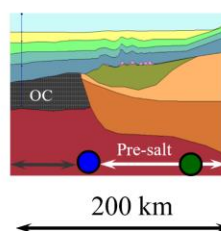
5E. GUMBO4



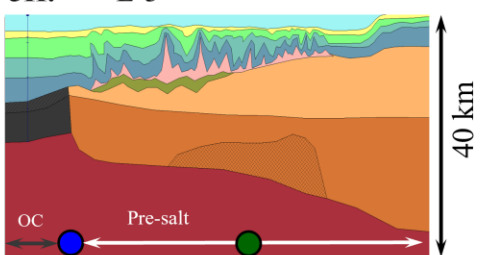
5F. L-1



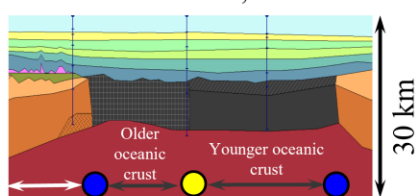
5G. L-2



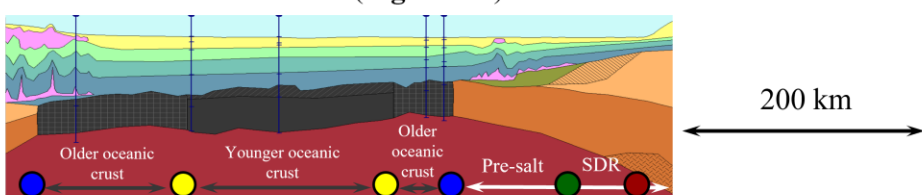
5H. L-3



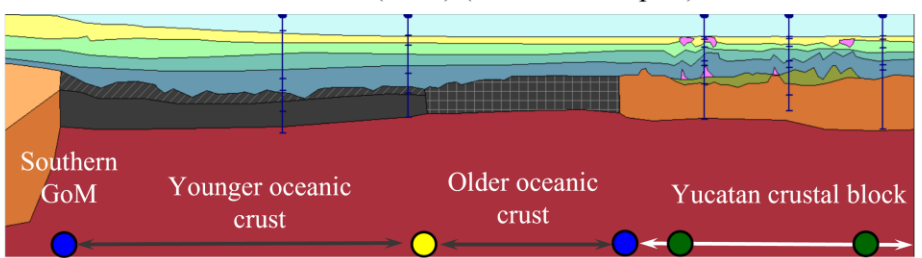
5I. Eastern GoM, N-S line



5J. TGS GIGANTE line (Figure 2A)



5K. Profile from Horn et al. (2017) (southwestern part)



Profile from Horn et al. (2017) (northeastern part)

overlap

